AN ABSTRACT OF THE THESIS OF

Chih-Ting Hsieh for the degree of Master of Science in Oceanography presented on June 5, 2009.

Title: Deconvolving the Sedimentary Phases of Barium Using Flow-Through Time-Resolved Analysis

Abstract approved: _____
Marta E. Torres and Gary P. Klinkhammer

The distribution of barite ($BaSO_4$) in marine sediments has long been studied as a proxy for paleoproductivity. While pure barite is known to be a stable mineral in oxic sediments, it is also known that variations in the Sr/Ba ratio influence its solubility and liability during early diagenesis. To extract this information we developed Flow-Through Time-Resolved Analysis (FT-TRA) technique coupled with Inductively Coupled Plasma Optical Emission Spectroscopy (ICP-OES) to continuously monitor the dissolution process using sequential leaching with deionized water (DIW), acidic acid (HNO_3), acidic hydroxylamine (NH_2OH) and diethylene triamine pentaacetic acid (DTPA) at controlled flow rate and temperature. We applied this technique to the analyses of barite samples and sediments from two contrasting basins in the California borderlands. To further understand various barium-carrying phases we analyzed foraminifera recovered from core tops from various locations around the world, using FT-TRA coupled with Inductively Coupled Plasma Mass Spectrometry.

Combined with available pore water data, our results provide a set of data that illuminates the nature (e.g. barite, carbonate, oxyhydroxide) and composition (e.g. relative concentrations of Sr, Ba and Ca) of barium-carrying phases to the sediment. We found the presence of a barium-carrying carbonate phase, hitherto unrecognized,

which is present both as disseminated carbonates in the sediment as well as overgrowths in foraminifera. This phase has various compositions, but in general contains significantly more barium than biogenic carbonate, and may be responsible for early diagenetic remobilization of barium as the pH of the sediment is lowered during oxic respiration.

The analytical technique and the results presented in this thesis provide the foundation for further investigations that can be used to constrain the barium geochemistry so as to fully exploit its application in a wide realm of studies.

Deconvolving the Sedimentary Phases of Barium Using Flow-Through Time-Resolved Analysis

by
Chih-Ting Hsieh

A THESIS

Submitted to

Oregon State University

in partial fulfillment of

the requirements for the

degree of

Master of Science

Presented June 5, 2009

Commencement June 2010

Master of Science thesis of Chih-Ting Hsieh presented on June 5, 2009

APPROVED:

Co-major professor, representing Oceanography

Co-major professor, representing Oceanography

Dean of College of Oceanic and Atmospheric Sciences

Dean of the Graduate School

I understand that my thesis will become part of the permanent collection of Oregon State University Libraries. My signature below authorizes release of my thesis to any reader upon request.

Chih-Ting Hsieh, Author

Dedicate to my parents, Wen-Chang and Shu-Jen,

who inspire me to explore the world.

ACKNOWLEDGEMENTS

I gratefully thank Andy Ungerer and Bobbi Conard, who taught me how to operate ICP-OES and ICP-MS and assisted me whenever I needed them. Thanks to June Padman, who taught me how to pick foraminiferal shells, and Alan Mix, who kindly provided me those foraminiferal samples. Margaret Saprrow and Frank Tepley helped me analyze the sediment and barite samples. Jesse Muratli helped me run microwave experiments to measure Ba contents in the sediment and Bart De Baere nicely provided me some of his foraminiferal data for my second chapter of the thesis. These people have significant scientific contributions to my thesis and many thanks to their technical support.

Many thanks are owed to Ahmed Rushdi who gave me a significant input on Flow-Through technique. Zanna Chase is a thoughtful and enthusiastic professor whom I admire and from whom I learned how to communicate with students when I was her TA. I am also thankful for Claire Reimers, Jennifer McKay, Alan Mix, James McManus and Fred Prahl for their helpful ideas toward my reaserch and cheer me up time after time.

I deeply appreciate Linda LaFleur and Lori Hartline who have warm hearts and always be there to help me. They supported me and provided me solutions when I had troubles in my daily life. Erica Schaefer was my first COAS friend who brought me to this kind and sweet COAS family. Greg Wilson, Dongwha Sohn, Maureen Davies, Rebecca Poulson and Robyn Matteson are my good friends who usually come by and refresh me away from work. Jesse Muratli, not only my labmate

but also “teamate”, who shares various flavors of tea with me every day. Gwenn Kubeck is my very good friend in COAS, who introduced me to know her family—her husband, Cosmo Prindle, and her sweet dog, Osa. Ruiqing Ye, Ruliang Liao and Wei Liu are my dear friends who often celebrate holidays with me and spend time together in cooking and exchanging recipes. I appreciate these friends very much. My life would be totally boring and miserable without their companionship in the past three years.

Bob Collier is the first professor in COAS that I heard of, thanks to Erica, when I was in Taiwan. He is a kind and considerate professor and a dog-lover as I am. I am thankful for him to give me a hand whenever I had difficulties in life or in academics. And his wife, Pat, treats me like I am one of her family members. I want to thank her for teaching me how to make an apple pie from scratch. I also enjoyed the time with their two dogs, Osito and Crystal, and one cat, Bisquick. They brought me lots of joy. It is never overstated to say that they are my second family in the U.S.

Many thanks are owed to Gary Klinkhammer, one of my advisors in COAS. He introduced me into the world of flow-through leaching technique, and was very patient to teach me during the stage of development of our technique. His wife, Susan, is a very nice person who welcomed me and made me feel like home when I first came to the U.S. I want to thank them for being so generous and kind to me.

The other advisor of mine, Marta Torres, is the woman who I admire and respect very much. I learned her persistent and strong faith when she knew her illness and fought for it. She balances her life between research and her family and

still has energy to make everyone laugh. Wherever she goes, the joy comes around her. She is my role model as a female oceanographer.

I would like to thank my parents, Wen-Chang Hsieh and Shu-Jen Chou, who support me no matter how bad the situation is. Without their believing in me, I may not be able to explore the world with confidence. Although my dogs, Mou and Pan, do not read, I still want to thank them for bringing me joy whenever I thought about them. They have accompanied me for about 14 years. I wish them healthy and happy forever.

Last but not least, I want to thank my beloved soon-to-be husband, Chao-Chin Yang, for always being there to support me. There is no one who brings me such comfort and happiness in my life and I might not accomplish this work without him.

TABLE OF CONTENTS

TABLE OF CONTENTS (CONTINUED)

LIST OF FIGURES

LIST OF FIGURES (CONTINUED)

LIST OF TABLES

Deconvolving the Sedimentary Phases of Barium Using Flow-Through Time-Resolved Analysis

Introduction

The utilization of barium (Ba) as a proxy for paleoproductivity has led to extensive efforts to better understand its behavior in the modern ocean by establishing the main carrier phases and their compositions, comparing it with multiple proxies in a variety of environments, documenting factors that control its preservation in sediment, and identifying complications to its application (Francois et al., 1995; Rutsch et al., 1995; Frank et al., 1995; Dymond and Collier, 1996; McManus et al., 1999; Klump et al., 2000; Fagel et al., 2004; Bernstein and Byrne, 2004; Reitz et al., 2004; Sternberg et al., 2005).

The occurrence of the stable mineral barite ($BaSO_4$) appears to be most closely linked to biological production (Bishop 1988; Dehairs et al., 1991; Paytan et al., 1996; Schroeder et al., 1997; Ganeshram et al., 2003), and studies of the fidelity of Ba as a paleoproductivity proxy have tended to focus on the flux and geochemistry of this phase. Barium, however, is also present in other forms (Dehairs et al., 1980; Collier and Edmond, 1984; Dymond et al., 1992; Schroeder et al., 1997; McManus et al., 1998), as well. Its association with oxyhydroxides, for example, has been postulated as an important source of barium to hemipelagic sediments (McManus et al., 1998). The contribution of these phases to the overall barium inventories and their behavior during diagenesis still remains unresolved. To fully exploit the potential of barium as a paleotracer, it is important to investigate the variation in Sr/Ba ratios of crystal barite, as it has a great influence on barite solubility and its

early diagenetic processes. In addition, the role of alternative barium carriers to the sediments (e.g. aluminum silicates, oxyhydroxides and carbonates) and their contributions to overall barium budget and burial efficiency need to be resolved (Figure 1.1).

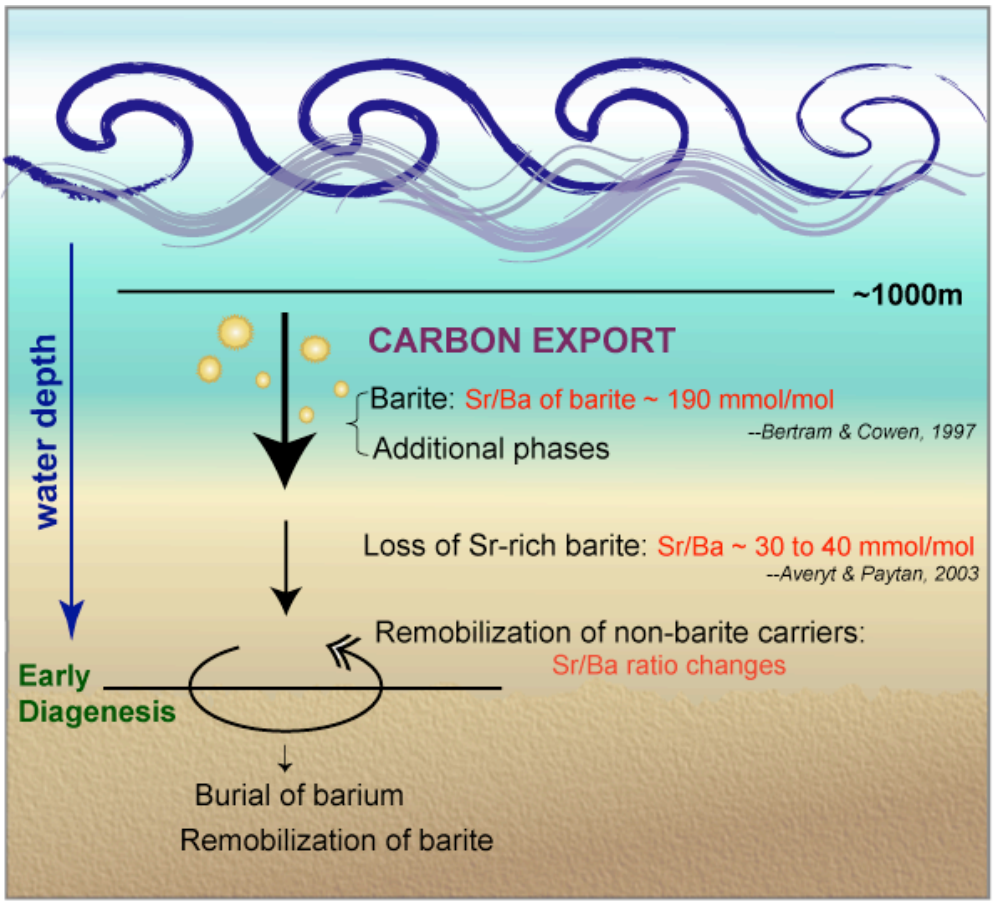

Figure 1.1: Cartoon illustrating the various components of the carbon cycle in which barium has been suggested as a proxy.

The techniques currently used to describe and quantify barium phases are all based on batch leaching techniques that define barium phases operationally, not chemically. Because during batch analyses each phase is characterized by a single-point measurement, variations due to phase heterogeneities cannot be resolved; nor

can the results of these experiments be related in any systematic way to what happens in nature. To overcome this problem we developed a new flow-through time-resolved analysis (FT-TRA) coupled with Inductively Coupled Plasma Optical Emission Spectrometry (ICP-OES), which allows complete monitoring of the dissolution of barite samples as each phase is sequentially leached with different reagents.

The first chapter of this thesis describes the FT-TRA and its applications to the study of barite and barium-bearing sediments to define the various Ba-carrying phases and their response to chemical treatments. Time-resolved analysis of the data stream allows us to monitor each single phase of barium dissolution. Analyses of barite samples recovered from a cold seep site show that our procedure results in dissolution of more than 85% of total barite, and also allows for identification and quantification of a highly soluble barite phase (Sr/Ba range from 90 to 210 mmol/mol) and a more refractory phase (Sr/Ba range from 25 to 70 mmol/mol). These results are consistent with previous findings that documented the existence of Sr-rich barite (Bertram and Cowen, 1997) and with our electron microprobe data that showed clear oscillatory zoning of the $(Ba,Sr)SO_4$. Unlike the barite sample, sediment samples collected from the vicinity of the seep sites did not show the presence of the high Sr/Ba phase. We might speculate that the highly susceptible Sr-rich barium phase present in the barite sample, dissolved during transport and early diagenesis at the sediment water interface, leaving a barite with a lower Sr/Ba ratio, as found in the sediment samples. This process is likely to be responsible for the decrease in the Sr/Ba ratios in barite during transport to the sediments, from the

extremely high values measured in samples recovered from the water column, to those found in the underlying sediment (Figure 1.1).

By applying our technique to sediment samples from different locations, we were able to identify different carrier phases for barium. For example, in the hemipelagic sediments from Santa Catalina basins, a fraction of the barium is clearly associated with oxyhydroxides; as the chromatograms for these sediments showed a simultaneous release of iron and barium during the hydroxylamine leach. These results are consistent with pore water data that show a release of barium concomitant with iron.

More surprisingly, however, we found that a large fraction of barium (40-60%) was leached from the Santa Catalina sediments with an acid treatment. Analyses of the Ba, Ca and Sr distributions in the acid treatments of Santa Catalina and San Clemente sediments, and the comparison with the composition of biogenic calcite and barite, point to the presence of a previously unrecognized barium-bearing inorganic carbonate phase. The presence of this phase may explain the observations of McManus et al. (1998) of a significant release of barium into the pore water when the sediments are not squeezed immediately after core recovery.

Further analysis of a series of foraminifera samples described in Chapter 2 also documents the presence of a non-biogenic barium-carrying phase, associated with shells recovered from areas of high barium flux to the sediments. The excess barium, which represents >90% of the barium on the shells, is leached after most of the biogenic calcium has dissolved, thus we postulate that it is associated with a

secondary carbonate phase, or overgrowth. The presence of these overgrowths on biogenic calcite appears to be a common feature of foraminiferal shells from the Equatorial Pacific, and other regions characterized by high barium concentration in the sediments, such as the Arabian Sea. Samples collected from the South Pacific, on the other hand, show a homogeneous Ba distribution within the shell, and Ba/Ca ratios that are consistent with those expected from live culture experiments. In all cases, our analyses show a simultaneous leaching of Ca and Sr, with a ratio consistent with that reported for foraminiferal calcite (Lea and Boyle, 1993), indicating that only barium is incorporated in the shell overgrowth in regions where there is a large barium flux to the sediments. The presence of a carbonate-bound barium phase in foraminifera is highly relevant for the application of Ba/Ca ratio as a circulation tracer and proxy for nutrients.

In summary, our results, combining with available pore water data, provide a set of data that illuminates the nature (e.g. barite, carbonate, oxyhydroxide) and composition (e.g. relative concentrations of Sr, Ba and Ca) of barium-carrying phases to the sediment. Furthermore, our results point to the presence of a barium-carrying carbonate phase, hitherto unrecognized, which is present both as disseminated carbonates in the sediment as well as overgrowths in foraminifera. This phase has various compositions, but in general it contains significantly more barium than biogenic carbonate, and may be responsible for early diagenetic remobilization of barium when the pH of sediment pore water decreases during oxic and suboxic respiration.

The analytical technique developed in this study, as well as the results presented in this thesis, provide the foundation for further studies that can be used to constrain the barium geochemistry so as to fully exploit its application in a wide realm of studies. Examples of potential future studies include:

1) Trace the behavior and significance of high strontium barite from the water column to the sediments by analyzing samples from sediment traps, core tops and downcore.

2) Further characterize the nature of the acid-leachable barium phase. This can be accomplished by implementing different leaching methods (e.g. using acetic acid, different temperatures and analytical runs) and by analyzing the eluates for anion composition.

3) Constrain the nature of Ba overgrowths in foraminifera by conducting a comprehensive analyses of foraminifera samples from a wider set of regions, and by tracing its distribution from the water column (using sediment trap samples), to the sediments (core top samples), and its fate during burial (by analyzing foraminifera samples downcore)

Additional applications of this technique include the characterization of carbonates and microfossils from areas of active seepage to evaluate whether the presence of overgrowths in the shells could be used as a tracer for fluid venting episodes in the past; and the characterization of barite recovered from diagenetic fronts to fully exploit their potential as tracers of fluid methane sources in continental margins.

Chapter 1

High-Resolution Leaching of Marine Barites and Sediments using Flow-Through Time-Resolved Analysis

Chih-Ting Hsieh, Marta E. Torres, Andy Ungerer and Gary P. Klinkhammer

2.1 Abstract

The distribution of barite ($BaSO_4$) in marine sediments has long been studied as a proxy for paleoproductivity. While pure barite is known to be a stable mineral in oxic sediments, it is also known that variations in the Sr/Ba ratio influence its solubility and liability during early diagenesis. This study quantifies these effects in natural samples for the first time and examines sediment samples for other potentially important carriers that might affect the cycling of barium in the oceans and thus our interpretation of its record in sediments. To extract this information we developed Flow-Through Time-Resolved Analysis (FT-TRA) technique coupled with Inductively Coupled Plasma Optical Emission Spectroscopy (ICP-OES) to continuously monitor the dissolution process using sequential leaching with deionized water (DIW), acidic acid (HNO_3), acidic hydroxylamine (NH_2OH) and diethylene triamine pentaacetic acid (DTPA) at controlled pressures and temperatures. The DIW leach revealed the presence of a highly soluble phase, with Sr/Ba ratios of 90-210 mmol/mol, which was eluted during the first 3 minutes, after which, ratios quickly reached an asymptotic value between 30 and 60 mmol/mol. Approximately 4% of the sample was removed with DIW and about 7% dissolved in subsequent HNO_3 leach with a Sr/Ba ratio of ~25 mmol/mol. Hydroxylamine in acetic acid leached an additional 7% with Sr/Ba ratios of 30-70 mmol/mol. The final DTPA leach dissolved up to 80% of the barite sample with Sr/Ba ratios of 30-60 mmol/mol.

FT-TRA of sediments from San Clemente and Santa Catalina basins revealed significantly different partitioning of barium: San Clemente sediment recovered near a cold seep most barium was leached as barite with DTPA, whereas in Santa Catalina sediment the largest fraction of barium was removed in the acid leach (40-60%). The prevalence of this previously unrecognized barium-rich carbonate phase was also apparent in the element-to-element analyses. Moreover, based on correlations between various elements monitored during our leaching experiments, it was clear that we can easily differentiate the barite-bearing sediment of San Clemente from the more typical margin sediment of Santa Catalina, opening the door for future proxy development. Our results highlight the value of FT-TRA for quantification of element substitution into barite, and for the identification of various carrying phases and their composition--phases that are clearly significant in the overall budget and burial efficiency of barium.

2.2 Introduction

Marine sediment contains a potential wealth of information regarding climate change, upper ocean fertility and carbon cycling through time. The difficulty in interpreting this record lies in the fact that only a small portion of the material escapes the upper 1000 meters and even less is ultimately buried. Moreover, diagenetic processes and advective transport of particles may have significant effects on the preserved biologic signal (Dymond et al., 1992; Paytan et al., 1993; Paytan and Kastner, 1996).

The accumulation of sedimentary barium has been recognized as a potential proxy for biological productivity for some time (Goldberg and Arrhenius, 1958) and extensive studies have been made to quantify this relationship (Dymond et al.,1992; Francois et al., 1995; Dymond and Collier, 1996; Ganeshram et al., 2003; Fagel et al., 2004). The underlying basis for this potential has always lain in the assumption that most sedimentary barium exists as barite ($BaSO_4$) (Bishop, 1988; Dehairs et al., 1990, 1992; Paytan et al., 1993; Paytan and Kastner, 1996; Paytan et al., 1998; van Beek et al., 2003; Averyt and Paytan, 2003), and studies of the fidelity of Ba as a proxy have focused on the flux and geochemistry of the highly crystalline barite. Unlike organic matter, which undergoes efficient diagenetic recycling on the sea floor, approximately 30% of barite flux is preserved in oxic environments (Dymond et al., 1992; Paytan and Kastner, 1996; Paytan et al., 1993, 1996b, 1998). Because barite is known to be highly refractory, previous paleoceanographic studies have used aggressive chemical methods to isolate the barite crystals. Studies that have attempted to quantify the amount of barium originating as barite and other different phases in sediments have used batch-leaching techniques that define barium phases operationally, not chemically (Table 2.1). During batch analyses each phase is characterized by a single-point measurement, and therefore variations due to phase heterogeneities cannot be resolved; nor can the results of these experiments be related in any systematic way to what happens in nature.

Table 2.1
Previous sequential leaching methods in batch experiments

Reference	Reagent (removed phases)
Dymond et al., 1992 [1]	Sediment trap sample is treated with pH5 acetic acid (carbonates), pH 9 sodium dodecyl (organic phase) and pH 5 hydroxylamine hydrochloride solutions (Fe-Mn oxyhydroxides), and then is analyzed by AAS. The sum of Ba in these extractions is subtracted from total Ba, measured by dissolution of a separate split with HF/HNO_3, to obtain the residual Ba (refractory phase) in the sample.
Schenau et al., 2001 [2]	Sediment sample (125 mg) is treated with NH_4Cl (barite), Na-citrate/$NaHCO_3$/Na-dithionite (Fe-Mn oxyhydroxides), Na-acetate/acetic acid, DIW, $HClO_4/HNO_3/HF$ (aluminosilicates), and then is analyzed by ICP-OES.
Rutten and de Lange, 2002 [3]	Sediment sample (250 mg) is treated with $MgCl_2$ (absorbed ions), NH_4Cl (barite), ascorbic acid/$NaHCO_3$/sodium citrate solution (oxides), NaAc (remaining carbonates), sodium dithionite/sodium citrate/sodium acetate solution (crystalline oxides), HF (clay minerals), HNO_3 (pyrite and organic bound metals) and $HClO_4/HF/HNO_3$ (residual minerals), and then is analyzed by ICP-OES. Called the BASEX method.
Gonneea and Paytan, 2006 [4]	Sediment sample (2-3 g) is treated with acetic acid (carbonates), sodium hypochlorite (organic bound element), hydroxylamine (Fe-Mn oxyhydroxides), HF/HNO_3 (aluminosilicates) and $HF/HNO_3/HClO_4$ solutions (refractory phase), and then is analyzed by ICP-OES.
Snyder et al., 2007 [5]	Sediments left from pore-fluid extraction are rinsed with DIW (remnant of interstitial water) three times, freeze-dried and ground. After that, sediment sample (100-200 mg) is treated with pH 5 $NaC_2H_3O_2$ (carbonates), HCl, DIW and Na_2CO_3 (barite), and then is analyzed by ICP-OES.

[1] Modified from Wefer et al., 1982; Robbins et al, 1984; Lyle et al, 1984.
[2] Modified from Schenau and De Lange, 2000.
[3] Modified from Ruttenberg et al, 1992; de Lange, 1992; Pruysers et al, 1993; de Lange et al, 1994; Kostka and Luther III, 1994; Rutten et al, 1999.
[4] Modified from Church, 1979; Collier and Edmond, 1984; Paytan et al, 1996b, 1996c; Eagle et al, 2003.
[5] Modified from Tessier et al., 1979; Li et al., 1995; Breit et al., 1995.

Here we describe a new Flow-Through Time-Resolved Analysis (FT-TRA) coupled with Inductively Coupled Plasma-Optical Emission Spectrometry (ICP-OES), which allows complete monitoring of the dissolution of barite and sediment samples as each phase is sequentially leached. Our experiments used the same phase-specific reagents that have been used previously in batch experiments. But the application of these reagents during controlled, time-resolved analysis allowed us to separate and quantify individual phases during the dissolution process. Applying this procedure to barites recovered from a cold seep site showed that we were able to characterize more than 85% of total barite. More importantly this novel approach allowed us to identify and quantify a highly soluble strontium-rich barite not previously resolved in the batch experiments.

2.3 Analytical development

2.3.1 System description

The flow-through module used here was previously developed for analysis of foraminifera, operated in line with Inductively Coupled Plasma Mass Spectrometry (ICP-MS), as described by Haley and Klinkhammer (2002). But we found that for barite and sediment the elements of interest and their concentrations were more suitable for optical emission (ICP-OES), so for this study the FT module was interfaced with the optical emission instrument, which also required new TRA software.

At the heart of the FT leaching system are off-the-shelf Dionex chromatographic components, most importantly an advanced gradient pump (AGP)

that delivers reagents from individual bottles through samples at constant flow rates. Samples are pre-loaded into 4 mm disposable syringe filters with 0.45 μm pore sized membrane made of inert fluorocarbon material. The Dionex AGP module with proportioning valve can be set to control the composition of the eluents, flow rate, and thus system pressure. Program settings are shown in Table 2.2. A heater is part of the FT module and in this case temperature was set at 80°C. The optimal wavelengths for each element (shown in Table 2.3) and the operating conditions for ICP-OES (listed in Table 2.4) were chosen to improve sensitivity and minimize interference.

Table 2.2
Time sequence of events of the five-day experiment programmed into the Dionex AGP

E1: 10 mM HNO3; E2: 0.02 M hydroxylamine in 25% (v/v) acetic acid; E3: 0.1 M DTPA (pH~10); E4: deionized water (DIW)

Time (min)	**%E1**	**%E2**	**%E3**	**%E4**	**Flow rate (ml/min)**	**Event**
1st day						
0.0	0	0	0	100	1.8	Labile(high-Sr) barite removal
30.0	0	0	0	100	1.8	
2nd day						
0.0	0	0	0	100	1.8	Labile(high-Sr) barite removal
29.0	0	0	0	100	1.8	
29.1	0	0	0	100	1.8	System rinse
30.0	0	0	0	100	1.8	
30.1	1	0	0	99	1.8	Carbonate phase removal
55.0	30	0	0	70	1.8	
60.0	30	0	0	70	1.8	
3rd day						
0.0	30	0	0	70	1.8	Carbonate phase removal
29.0	30	0	0	70	1.8	
29.1	0	0	0	100	1.8	System rinse
30.0	0	0	0	100	1.8	
30.1	0	100	0	0	0.2	Oxide and metal phase removal
60.0	0	100	0	0	0.2	
4th day						
0.0	0	100	0	0	0.2	Oxide and metal phase removal
29.0	0	100	0	0	0.2	
29.1	0	0	0	100	1.8	System rinse
30.0	0	0	0	100	1.8	
30.1	0	0	100	0	0.2	Refractory(low-Sr) barite removal
60.0	0	0	100	0	0.2	
5th day						
0.0	0	0	100	0	0.2	Refractory(low-Sr) barite removal
30.0	0	0	100	0	0.2	

Table 2.3

Selected wavelength for each element based on maximum sensitivity and minimum interference

Element	Wavelength (nm)
Na	589.592
Ba	455.403
Sr	421.552
Ca	317.933
Al	308.215
Mg	279.553
Fe	259.940
Mn	257.610

Table 2.4

Operating characteristics for Teledyne Leeman Prodigy ICP-OES

Parameter	Optimum
Radio-Frequency (RF) Power	1.3 kW
Coolant Flow Rate	18 LPM
Auxiliary Gas Flow Rate	0.3 LPM
Nebulizer Flow Rate	34 PSI
Integration Time	2 seconds
Time-Resolved Analysis View (For all method lines)	Axial
Spectrometer Temperature	35 °C

2.3.2 Samples and standards

This project took advantage of a collection of cold seep barites, recovered from the San Clemente fault zone by Torres et al. (2002). The barite samples were ground using an agate mortar and pestle. Reagent grade quartz distilled 1% HNO_3 was used to prepare standards and blanks. We gravimetrically prepared a standard stock solution containing Ba, Ca, Mn, Na (1 ppm), Sr, Mg (0.1 ppm), Fe and Al (0.5 ppm) to calibrate the ICP-OES.

Because the standards are used to calibrate the instrument during the various leaching steps, it was deemed impractical to prepare matrix-matched standards for each step. We thus evaluated the effect of hydroxylamine (NH_2OH) and diethylene triamine pentaacetic acid (DTPA) on the OES response independently relative to that of a 1% HNO_3. During the NH_2OH and DTPA leaching steps, deionized water (DIW) was added to the eluates (DIW : eluate = 8 : 1) before the fluids went into ICP-OES (as shown in Figure 2.1) because we found that the higher concentrations of these reagents as used for leaching made the plasma unstable. We measured the signal intensity using both diluted and undiluted NH_2OH and DTPA solutions and found that matrix effects of NH_2OH and DTPA from ion suppression in the plasma were generally less than ±5% (Figure 2.2).

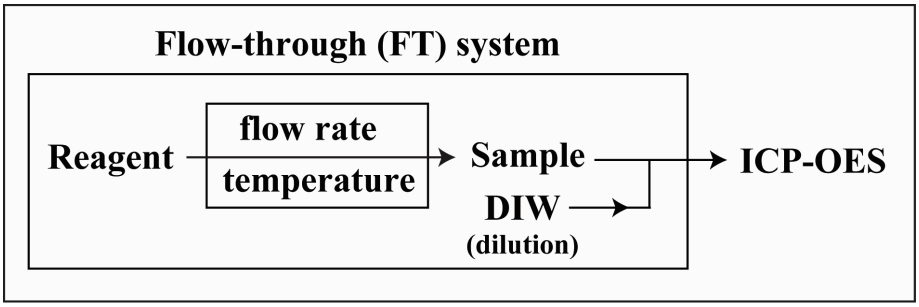

Figure 2.1. Flow diagram of the FT-ICP-OES setup used in our experiments. Reagent of constant flow rate and temperature flows through the sample column and is then diluted with DIW before going into ICP-OES during NH_2OH and DTPA steps.

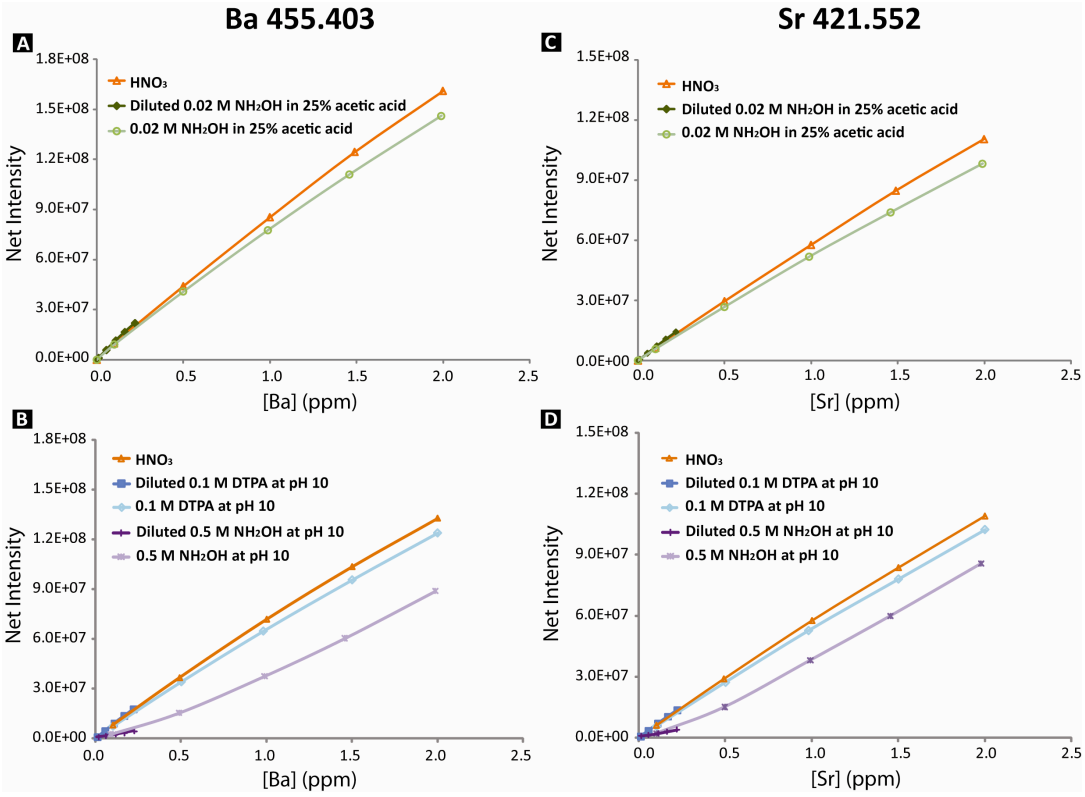

Figure 2.2. Matrix effects on Ba and Sr in NH_2OH and DTPA solutions compared to 1% HNO_3, considered to be the idea plasma matrix.

2.3.3 Procedure

Before starting each analysis, the system was allowed to reach the operational temperature of 80°C, which was maintained throughout the runs. During this time, 1% HNO_3 was used to rinse the system lines. A well-ground barite sample (100-200 μg) was loaded in the sample, and subjected to sequential leaching with DIW, HNO_3, NH_2OH and DTPA, as outlined in Table 2.5. The system was rinsed with DIW for one minute between every reagent change to prevent cross-contamination. We also ran a final rinse with 1% HNO_3 (10 minutes) and DIW (5 minutes) at the end of each run to clean the system walls.

Table 2.5
Procedure of the five-day experiment by FT leaching technique*

Day	Procedure
1st day	Sample leached with DIW for 30 minutes and left overnight.
2nd day	Sample leached with DIW for 29 minutes. Lines rinsed with DIW for one minute. Sample leached with 0.1 mM HNO_3 and then ramping up linearly to 3 mM over 25 minutes. Sample leached with 3 mM HNO_3 for another five minutes, and left overnight.
3rd day	Sample leached with 3 mM HNO_3 for 29 minutes. Lines rinsed with DIW for one minute. Leached sample with 0.02 M NH_2OH in 25% (v/v) acetic acid for 30 minutes, and left overnight.
4th day	Sample leached with 0.02 M NH_2OH in 25% (v/v) acetic acid for 29 minutes. Lines rinsed with DIW for one minute. Sample leached with 0.1 M DTPA (pH~10) for 30 minutes, and left overnight.
5th day	Sample leached with 0.1 M DTPA for 30 minutes.

* The flow rates of DIW and HNO_3 were set at 1.8 ml/min, whereas the flow rates of NH_2OH and DTPA were set at 0.2 ml/min in order to attain better phase separation. For NH_2OH and DTPA leachates, DIW was pumped via internal standard position at 1.6 ml/min flow rate to mix with the eluate from the sample valve in order to reduce the matrix effect and produce the correct flow rate (1.8 ml/min) for the ICP-OES nebulizer.

The first leaching step was aimed at removing the most labile phases (high-Sr) of barite by leaching with DIW, which is slightly acidic (pH~5). The second leaching step was formulated to dissolve carbonates with nitric acid (Haley and Klinkhammer, 2002). The concentration of HNO_3 was carefully controlled so as not to over-leach the barite because our preliminary results had shown that 100 mM HNO_3 could dissolve up to 40% of the barite. We avoided this potential problem by using a minimal amount of acid: 0-3 mM HNO_3 for the first 25 minutes, followed by 3 mM HNO_3 for another 5 minutes.

The next step of the barite leaching procedure was removal of iron-manganese oxyhydroxides with NH_2OH. As shown in Table 2.1, the NH_2OH solutions used by previous investigators to reductively remove oxyhydroxides are vastly different. (Boyle, 1981) used the most aggressive solution (~0.685 M NH_2OH in 40% NH_4OH). Work by other investigators (e.g. Rutten and Lange, 2002)would suggest that this reagent is likely to dissolve some of the barite due to its high pH, and indeed we found in our preliminary experiments that leaching barite with this solution led to significant dissolution (15-25%). This solution also resulted in significant signal suppression (Figure 2.2). Because of these issues we went on to test a solution containing 0.02 M NH_2OH in 25% (v/v) acetic acid, as recommended by Church (1979) and Paytan et al. (1993). We found that this solution produced minimum matrix effects and did not attack barite so it was adopted for our procedure.

We used DTPA to dissolve refractory barite. Temperature plays an important role on barite dissolution, with the rate constant of barite dissolution at 80°C almost six times higher than at 40°C (Dunn and Yen, 1999). The pH of the solution is also important; under a high-pH condition (pH>12) each DTPA molecule is able to chelate one Ba^{2+} ion (Martell and Hancock, 1996). Unfortunately we found in our experiments that the plasma in the ICP-OES became unstable at pH>10; therefore, we chose a DTPA solution adjusted to pH 10, which gave good chelating ability but did not degrade plasma stability. Finally, to find the lowest, effective DTPA concentration, we placed equal amounts of cold seep barite in four Teflon® beakers filled with a range of solutions (0.05 M, 0.1 M, 0.2 M and 0.5 M) adjusted to pH 10. These test samples were heated to 80°C and stirred constantly for one day. The 0.05

M solution gave incomplete dissolution while we obtained >85% dissolution with 0.1 M DTPA, with no significant increase at higher concentrations. We thus used 0.1 M DTPA for our experiments because it had the smallest matrix effect in the plasma. We also knew from previous studies by other investigators (Putnis et al., 1995) that higher DTPA concentrations can cause passivation of the barite surface.

2.4 Results and discussion

We first analyzed several barite samples recovered from cold seeps along the San Clemente escarpment using the FT-TRA technique, and showed that the chemical procedure we had developed could attain complete dissolution. The Sr/Ba ratios we found in these samples are summarized in Table 2.6 and the percentage of Ba dissolution is shown in Figure 2.3. In these experiments the barites were first leached with DIW (pH 5) for 30 minutes; less than 3% of the barite dissolved in this step. Acid leaching of the samples with HNO_3 removed an additional ~7%, and this phase has a Sr/Ba ratio ~25 mmol/mol. Hydroxylamine in acetic acid leached another ~7% with Sr/Ba ratios of 30-70 mmol/mol in this step. The final DTPA leach contained up to 80% of the sample and this final fraction had Sr/Ba ratios ranging from 30 to 60 mmol/mol.

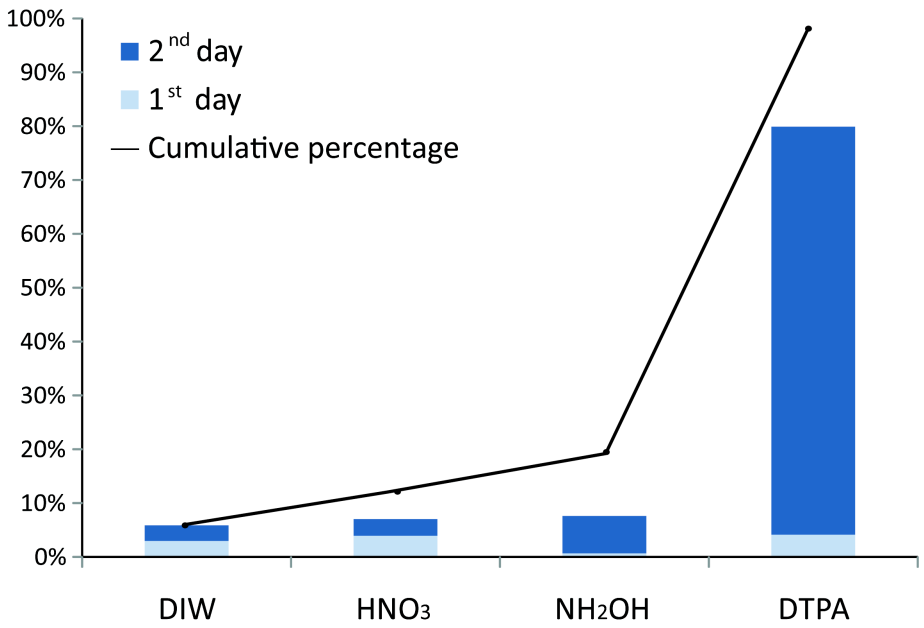

Figure 2.3. Cumulative percentage of dissolved barite. Light color represents the first day of each reagent; the dark color represents the second day of each reagent after sitting overnight.

A comparison of results for typical FT-TRA in barite analyses with traditional batch method by Averyt and Paytan (2003) is shown in Table 2.6. We found evidence for a barite fraction with an extremely high Sr/Ba ratio (110 mmol/mol) that dissolved readily upon initial contact with DIW. This highly soluble fraction was followed by dissolution of a more abundant phase having a nearly constant ratio of approximately 24-42 mmol/mol, except for two additional phases with Sr/Ba ratios ranging from 60 to 70 mmol/mol, which appeared at beginning of the NH_2OH and DTPA leaches.

Table 2.6
Sr/Ba, Sr/Ca and Ba/Ca ratios in barite samples, showing the variability among various eluents and published literature values.

	Sr/Ba (mmol/mol)	Sr/Ca (mol/mol)	Ba/Ca (mol/mol)	Reference
DIW	110 and 30-40	0.03	0.73	This study
HNO_3	24-26	nd	nd	
NH_2OH	32-69	nd	nd	
DTPA	34-63	1.2	21	
--	23-40	11-16	330-670	Averyt and Paytan, 2003

* nd: not detectable due to low Ca concentrations in barite.

The Sr/Ba ratios of the refractory barites we found in our FT-TRA leaching experiments are consistent with the findings of Averyt and Paytan (2003); however, our Sr/Ca and Ba/Ca ratios are considerably lower (Table 2.7), indicating generally higher Ca concentrations in our barites. The rather large offsets between these methods are consistent with collateral dissolution of the more soluble barite phases during separation of barite crystals from sediment using traditional aggressive batch dissolution methods.

Table 2.7

Comparison of Sr/Ba, Sr/Ca and Ba/Ca ratios of foraminiferal shells with literature values.

Sr/Ca (mmol/mol)	Ba/Ca (mmol/mol)	Sr/Ba (mol/mol)
1.16-1.5 [a]	0.5-5.0 [b]	230-3,000 [a,b]
1.3 [c]	1.7 [c]	750 [c]

[a] Brown and Elderfield, 1996.
[b] Lea and Boyle, 1992.
[a,b] calculated from literature values
[c] this study

We subjected several sample types to FT-TRA in an attempt to identify all significant barium phases: (1) sediment samples (~1 mg each) collected in the vicinity of a barite edifice in the San Clemente seep, (2) more typical margin sediment from the Santa Catalina Basin, and (3) a foraminiferal sample (~10 tests of *G. ruber*) randomly picked from the core top sediment in South Pacific (KN7812-17BC 0-5 cm at 49.552°S-179.702°W). Sediment samples were treated with the same five-day procedure as barite analyses using FT-TRA coupled with ICP-OES, while the foraminiferal sample was treated with HNO_3 and measured using FT-TRA coupled with ICP-MS (more details in Chapter 2). Data from the foraminiferal analysis will be used in the subsequent discussion as a reference material for biogenic calcite to compare to barite and the two sediment samples.

All data presented here were corrected for salt contribution. The FT-TRA software accounts for clay contamination by following aluminum concentrations and correcting ratios by using standard metal/Al ratios in aluminosilicates. Barium contributed from aluminosilicate carriers was only significant in Santa Catalina sediment sample in the DIW and HNO_3 leaches (~10% each), which has been corrected using the Ba/Al ratio of 0.0075 (Dymond et al., 1992), while barite and San Clemente sediment samples were not corrected due to the negligible amount of Ba contributed from aluminosilicates (<1%).

2.4.1 Water leach high-strontium barite

Repeated analysis of the cold seep barite showed the presence of a phase with Sr/Ba ratios ranging from 90 to 210 mmol/mol. Dehairs et al. (1980) were the first to propose that barites with Sr/Ba ratios in excess of 200 mmol/mol may occur in the upper water column. Such phases were subsequently documented by Bertram and Cowen (1997) in zones of high biological productivity. A phase fitting this description was leached from our cold seep barites with DIW: a result that demonstrates its extremely high solubility and potential lability during sediment diageneses (Figure 2.4). SEM analyses of these same cold seep barites confirm the presence of bands of high strontium barite (Figure 2.5), as well as illustrate the highly heterogeneous nature of the crystal composition. In quantitative terms the high strontium phase corresponds to only a small fraction of these barites (<1%). In fact, as a result of the small size of this fraction, sample heterogenity, and small sample size, our leaching experiments did not show the presence of this extreme phase every time. Nonetheless, taken as a whole, our results indicate that care must be taken when preparing barite samples for complete analysis to avoid dissolving this highly soluble phase.

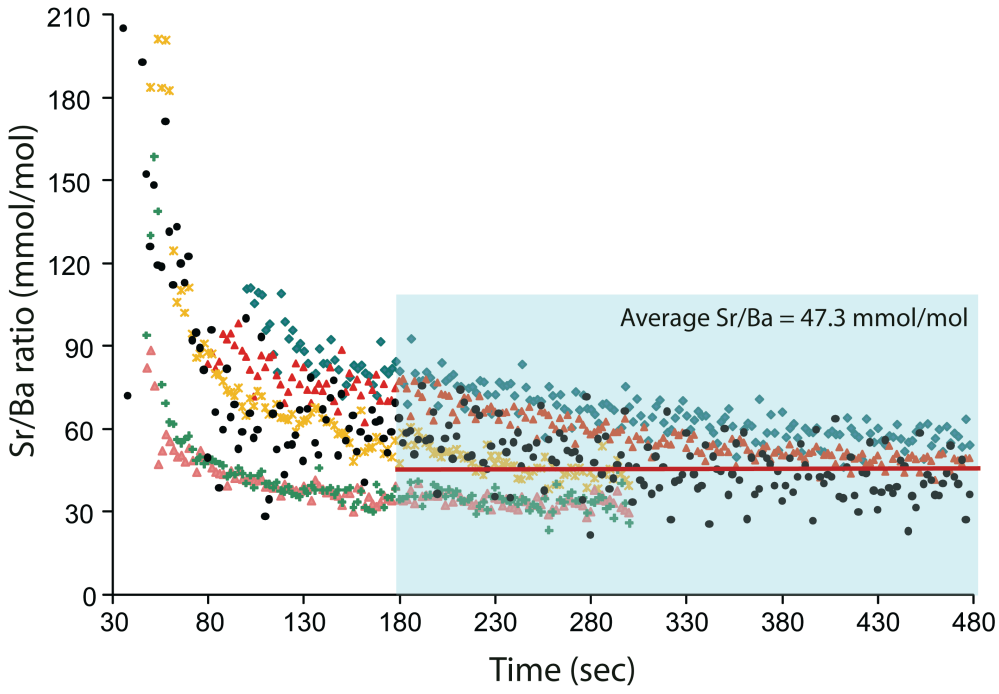

Figure 2.4. Sr/Ba ratios of a series of cold-seep barite samples. Parts of these barites have Sr/Ba ratios as high as 210 mmol/mol. Solubility is directly related to Sr/Ba and barite with the highest ratios dissolve in the first three minutes of a pH 5 DIW leach; after the high-Sr phases are removed, barites only have ratios of approximately 30 to 60 mmol/mol.

After dissolution of the Sr-rich phase, the Sr/Ba ratio of the bulk of the crystal shows values from 30 to 60 mmol/mol, ratios which were also found by Electron Microprobe analyses of these same barites (Figure 2.5), and which has been documented previously with barites recovered from a wide range of marine settings (Averyt et al., 2003; van Beek et al., 2003). Our results are the first experiments to quantify the complete range of Sr variability and associated elemental associations in marine barites.

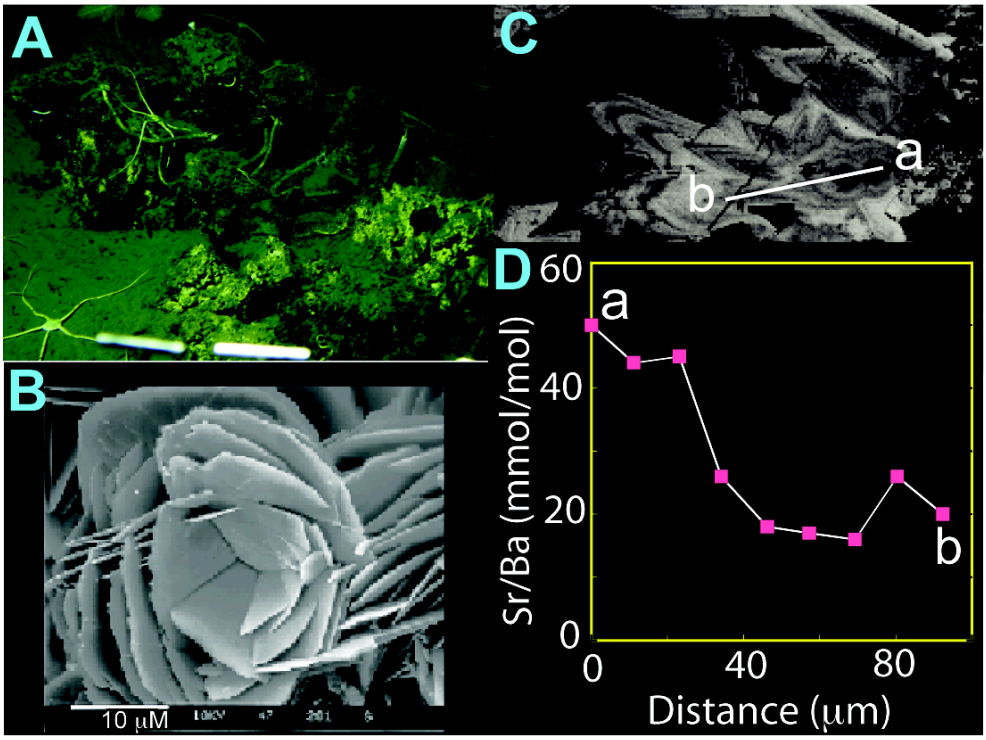

Figure 2.5. A) Picture of San Clemente scarp seeps, indicating the location where the cold seep barites for this study were collected. B) SEM image of the barite crystals, C) Backscattered electron image showing transect a-b. Dark areas are more Sr-rich. D) Sr/Ba ratios along a-b illustrating the variability of Sr.

Previous studies have shown that San Clemente sediment recovered in the vicinity of the barite chimneys at cold seep sites contains a significant fraction of microcrystalline barite crystals in a silty clay host sediment (Torres et al., 2002; McQuay et al., 2008). The FT-TRA of San Clemente sediments yielded 3 to 6% barium during the combined water rinses, in agreement with the fraction leached from pure barite. In analyses of various samples of Santa Catalina sediment, 10-20% of the barium was leached during the water rinse. These data are all corrected from any barium present in residual pore water using sodium data.

2.4.2 Acid leach

Treatment of barite with nitric acid dissolved 7 to 10% of the barite, and similarly, the San Clemente sediments yielded 9 to 11% of barium during the acid leach. In contrast Santa Catalina sediments had a much larger fraction of the total barium (40 to 60%) leached during the acid treatment (Figure 2.6), suggesting the presence of a Ba-rich carbonate phase. To further evaluate the nature of this phase, we analyzed the strontium, barium and calcium distributions among each of the phases sequentially leached during the FT-TRA of the sediments and compared them with the results for barite and foraminiferal samples, which constitute two of the potential endmember phases (Table 2.8). The correlations among Sr, Ba and Ca of foraminifera, barite and sediments from San Clemente and Santa Catalina basins in water and acid leaches obtained during the second day of FT-TRA are presented as Sr-Ca (Figure 2.7), Sr-Ba (Figure 2.8) and Ba-Ca (Figure 2.9). The results from these experiments show that the foraminiferal sample had Sr/Ca, Sr/Ba and Ba/Ca ratios that are in agreeement with the literature values for pristine biogenic calcite and can be viewed as a reference for this phase. For the barite endmember we use the value obtained from the analysis of pure barite using the same procedure as the analyses of Santa Catalina and San Clemente sediments. We found that recovery was not significantly different when using 3mM or 10 mM HNO_3.

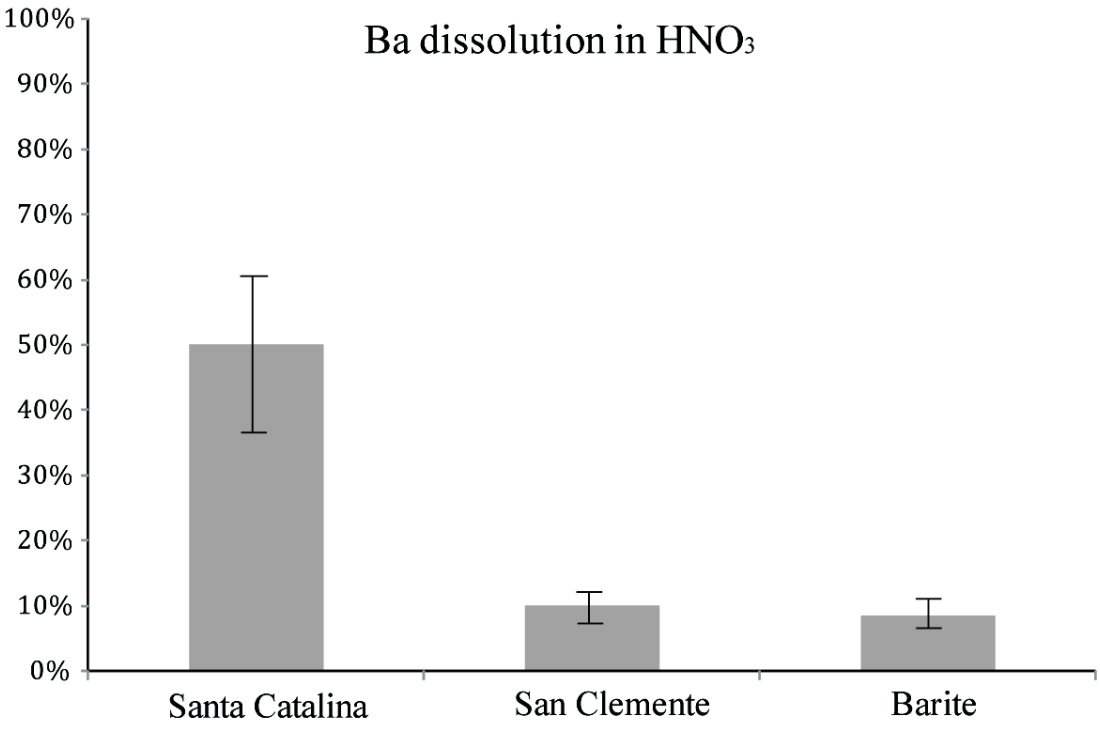

Figure 2.6. Histogram of barium dissolution during the acid leach for barite (n = 3 using both 3 mM or 10 mM HNO_3), Santa Catalina (n = 4) and San Clemente (n = 4) sediment samples. The acid-soluble fraction was a relatively large percentage of total barium in Santa Catalina sediment (~50%) compared to barite and San Clemente sediment (~10%).

Table 2.8. Sediment composition in San Clemente and Santa Catalina Basins

	San Clemente	Santa Catalina	Reference
Location	32.215°N, 117.719°W	33.236°N, 118.632°W	McQuay et al., 2008; Torres et al., 2002
Water depth (m)	1819	1325	
% Ba in the sediment	18	0.14	
% TOC	--	5.8	
% $CaCO_3$	--	16	
% Ba (DIW)	3	8-20	This study
% Ba (HNO_3)	7-12	40-60	
% Ba (NH_2OH)	4	3	
% Ba (DTPA)	80	15-30	

Santa Catalina sediment (Figure 2.7B) had Sr/Ca ratios within the range of foraminiferal calcite (Figure 2.7A), indicating that sedimentary Sr here is dominated by biogenic calcite. Barite (Figure 2.7C), on the other hand, had a Sr/Ca ratio of 27 mmol/mol in DIW. During the acid treatment of barite, there was not enough calcium released to accurately estimate this ratio, but it is >100 mmol/mol. In both leaches, the Sr/Ca ratio is one to two orders of magnitude higher than foraminiferal calcite. Since barite is very abundant in the San Clemente sediments (~18% Ba), we would expect to see similar or lower ratios than that of barite (27 mmol/mol), if only barite and biogenic carbonate (1.3 mmol/mol) were being leached by these eluents. However, we observed higher Sr/Ca ratios in both the DIW (64 mmol/mol) and HNO_3 (235 mmol/mol) fractions (Figure 2.7D), which suggests the presence of another labile phase(s) in San Clemente sediment associated with inorganic carbonate. This conclusion is still uncertain, however, and needs to be verified with additional leaching experiments. Nonetheless, we can use this preliminary information to construct a first-order approximation of the composition of the barium carriers in these sediments. Figure 2.10 shows the distribution of Sr/Ca, Sr/Ba and Ba/Ca ratios in foraminifera, barite and a postulated inorganic carbonate phase that is represented by the composition of the acid leaches from San Clemente sediments samples. Relative to these phases, we can see that Sr/Ca in Santa Catalina sediments can be readily explained as coming from the dissolution of biogenic carbonate.

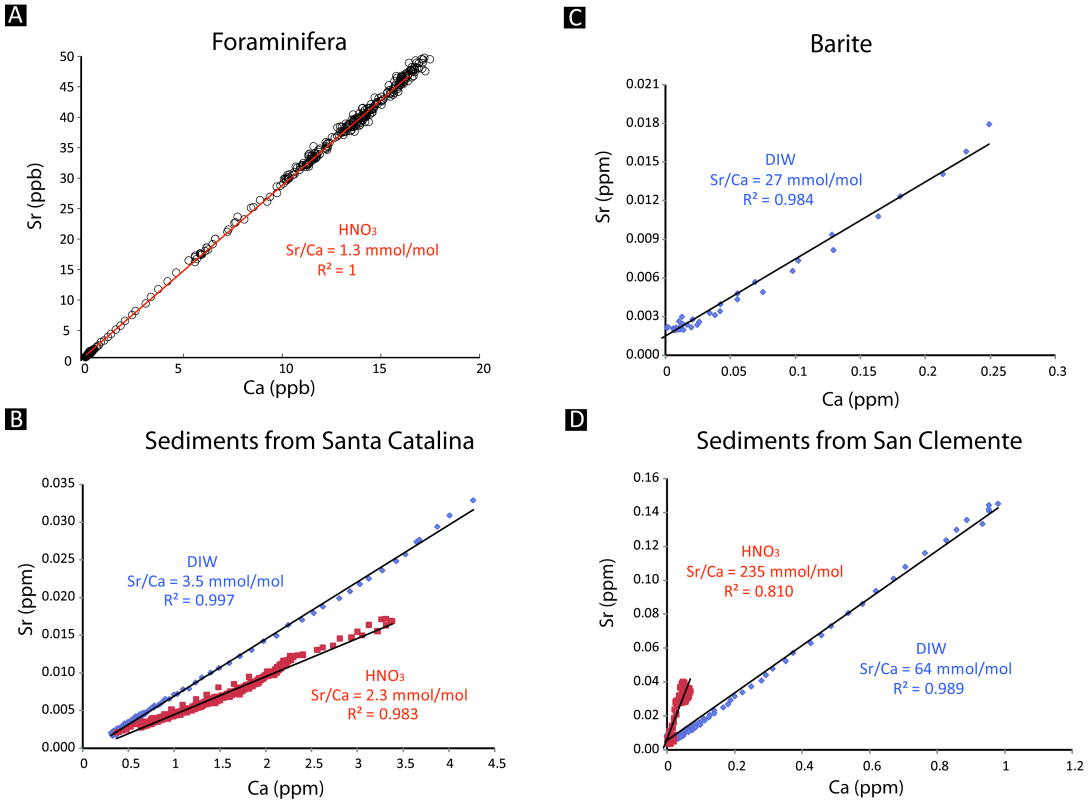

Figure 2.7. Sr vs. Ca plots of FT-TRA data from foraminifera, barite, and sediments from Santa Catalina and San Clemente basins using DIW and HNO_3. The excellent correlation in each of the eluents demonstrates the potential of this technique to separate and quantify various phases based on their susceptibility to dissolution.

Sr/Ba ratios of our barite samples (Figure 2.8C) leached with DIW and HNO_3 are consistent with microprobe analyses of the barite sample and are in agreement with Averyt and Paytan's (2003) results. Santa Catalina sediment (Figure 2.8B), on the other hand, has Sr/Ba ratios 10 times higher than the ratio of barite and 1000 times lower than the ratio of foraminifera in the acid treatment (Figure 2.8A). We conclude that neither foraminifera nor barite is the major source of Ba in the acid-soluble portion of Santa Catalina sediment. This result is also consistent with the presence of a carbonate fraction with a high Sr/Ca ratio, similar to what was deduced

for San Clemente. Accordingly, we postulate that the excess barium in this sediment is attributed to an inorganic carbonate phase, consistent with our observation that approximately 50% of the total barium from San Clemente sediment dissolved with nitric acid. Thus, the observed Sr/Ba ratio in these sediments can only be explained by a mixture of foraminiferal and inorganic carbonates, with a larger contribution of the inorganic carbonate, as illustrated in Figure 2.10B.

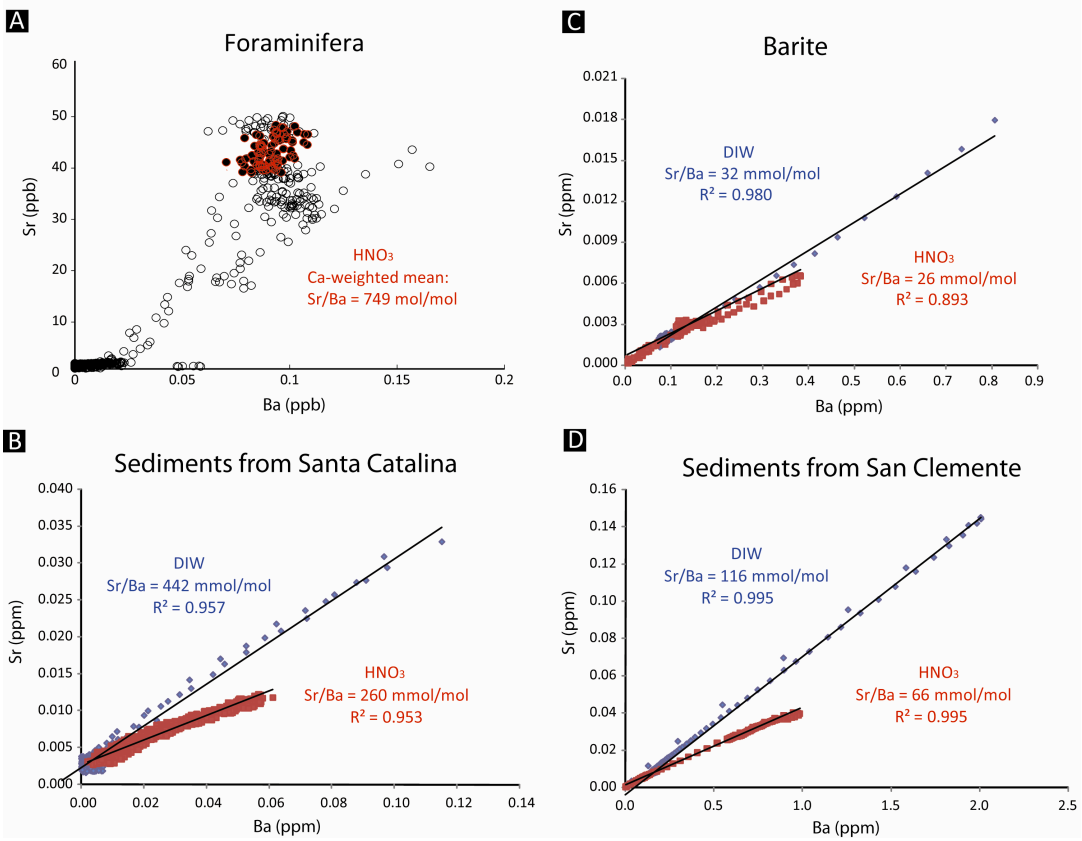

Figure 2.8. Sr vs. Ba plots of FT-TRA data from foraminifera, barite, and sediments from Santa Catalina and San Clemente basins using DIW and HNO_3. The amount of barium leached from the sample of foraminifera (0.2 ppb) was too small to allow for an accurate estimate of the Sr/Ba ratios using ICP-OES, therefore the foraminiferal sample was analyzed by ICP-MS and estimated using a Matlab-based software to yield the biogenic ratio (details in Chapter 2). This ratio is more than three orders of magnitude higher than the ones observed in barite and sediment samples.

Little of the total Ba in Santa Catalina sediment resides in pristine biogenic calcite because the Ba/Ca ratio (~8 mmol/mol in Figure 2.9B) is approximately three orders of magnitude higher than the ratio for foraminiferal calcite (Figure 2.9A). The Ba/Ca ratio in Santa Catalina sediment is, moreover, two orders of magnitude lower than barite (Figure 2.9C). We postulate that the Ba/Ca ratio in Santa Catalina sediment is dominated by a Ba-rich carbonate phase; this is as also apparent in Sr/Ca (Figure 2.10). This value it is still one order of magnitude higher than the Ba-rich carbonate phase present in formainifera from the Equatorial Pacific reported in another part of this study (Chapter 2). San Clemente sediment (Figure 2.9D) has a similar albeit somewhat lower ratio (547 mmol/mol) than barite in the water leach, however, we observed a higher ratio of 3800 mmol/mol in the beginning 10 minutes of acid treatment, which could also result from a hitherto unknown Ba-rich carbonate phase. Therefore, we believe this to be an inorganic barium-rich carbonate such as that present in San Clemente. The first 10 minutes of acid leach of the San Clemente sediment revealed a phase with a Ba/Ca ratio of 3800 mmol/mol (Figure 2.9D), which we postulate corresponds to the endmember carbonate phase, the remaining of the acid leach, has Ba/Ca ratios (550 mmol/mol) that are similar to those of the barite endmember (800 mmol/mol), and probably represent leaching of the barite present in these samples.

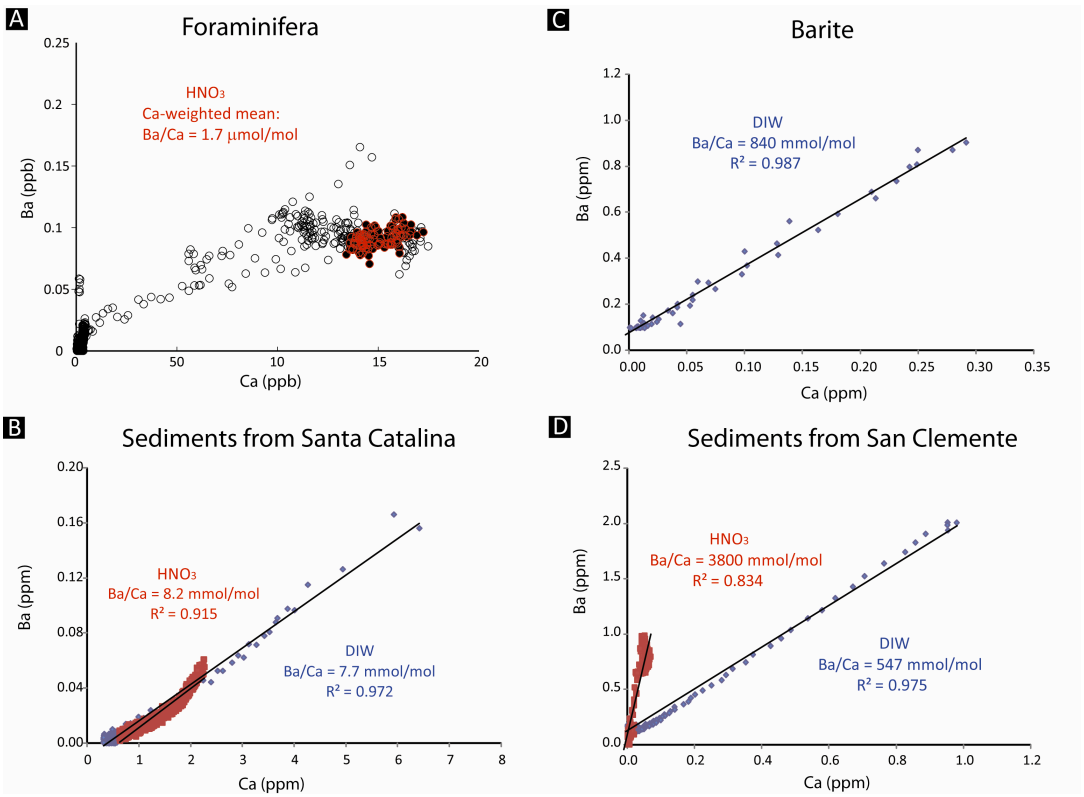

Figure 2.9. Ba vs. Ca plots of FT-TRA data from foraminifera, barite, and sediments from Santa Catalina and San Clemente basins using DIW and HNO_3. The amount of barium (~0.2 ppb) is too low or an accurate estimate of the Ba/Ca ratios in foraminifera using ICP-OES, therefore the foraminiferal sample was analyzed by ICP-MS and was estimated using a Matlab-based software program to yield the biogenic ratio (details in Chapter 2). The Ba/Ca ratios of Santa Catalina sediments are three orders of magnitude higher than the ratio in foraminifera and approximately two orders of magnitude lower than the ones in barite and San Clemente sediments.

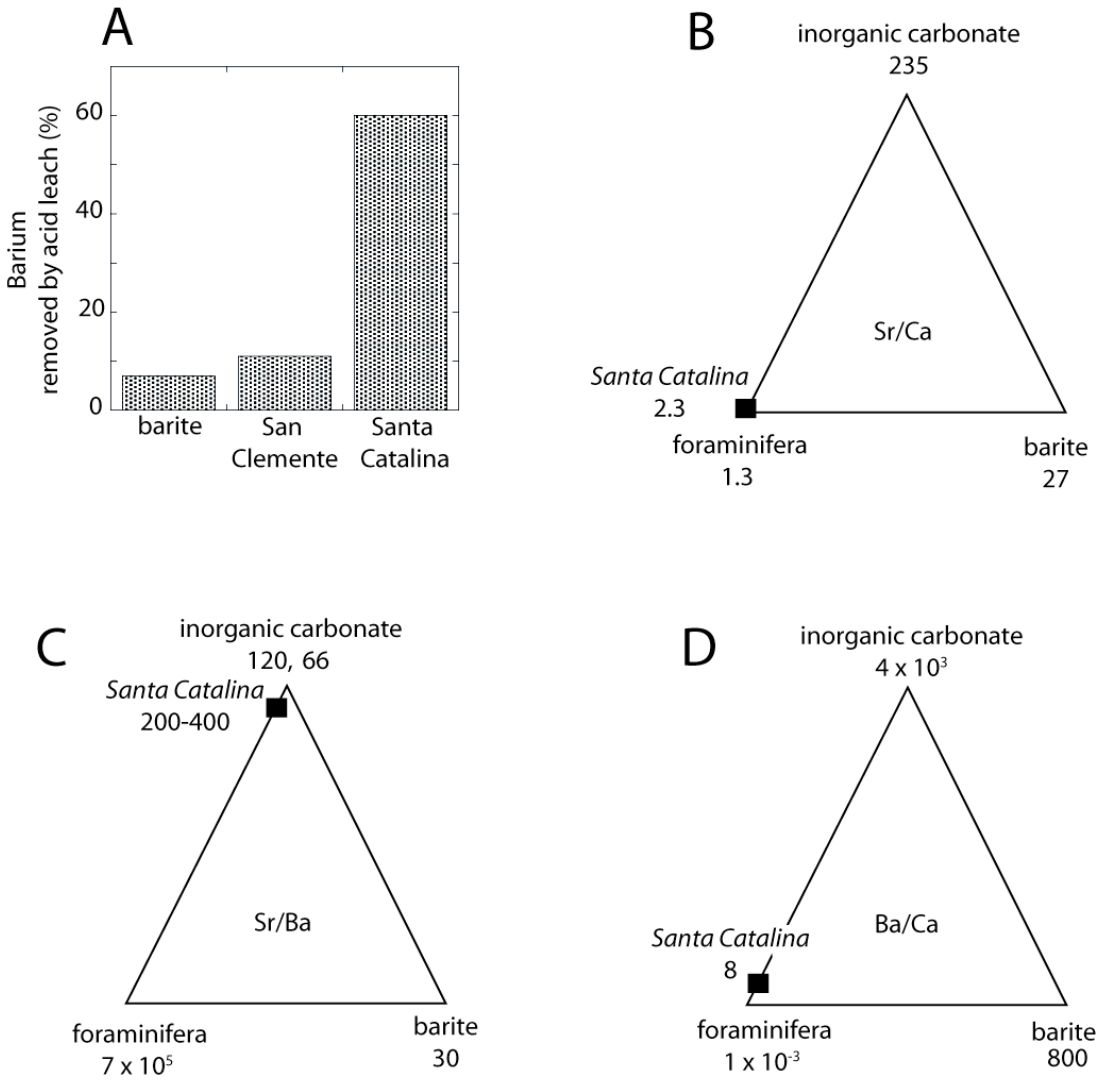

Figure 2.10. Distribution of Sr/Ca, Sr/Ba and Ba/Ca ratios in foraminifera (mmol/mol), barite and a postulated inorganic carbonate phase that is represented by the composition of the acid leaches from San Clemente sediments samples. Relative to these phases, we can see that the Sr/Ca in the Santa Catalina sediments can all be explained as resulting from dissolution of biogenic carbonate. However, a significant fraction of the barium is leached with the acid rinse (panel A), suggesting the presence of an additional barium-bearing carbonate phase. There is a pronounced enrichment of barium in this phase (panel C, 200-400 mmol/mol), which we postulate is responsible for the high barium dissolution by acid leach (panel A).

In summary, monitoring the chemical composition of these two contrasting sediment samples in the acid treatment allows us to identify distinct barium-carrying phases. Whereas only 11% of the barium in San Clemente sediment is leached with HNO_3, which mostly corresponds to leaching of barite crystals, the composition of this eluent indicates that in addition to barite, an inorganic carbonate phase with Sr/Ca ratios ranging from 60 to 235 mmol/mol is enriched in barium, with a Ba/Ca ratios as high as 3800 mmol/mol. In Santa Catalina sediment, which is devoid of marine barite contribution, the inorganic carbonate phase contributes to ~50 % of the total barium with a Ba/Ca ratio of ~8 mmol/mol.

2.4.2.1 Significance of this phase

In a thourough investigation of pore water data from the California margin, McManus et al. (1998) concluded that under suboxic diagenetic conditions, solid phase barium preservation may be reduced. Two mechanisms were put forward by these investigators to explain their data: 1) there are different solid phases of barium (or barite) arriving at the seafloor, and 2) that diagenesis in California margin sediments leads to enhanced remobilization of the primary Ba-containing phase resulting in high pore water barium concentrations in sulfate-bearing pore waters. Our results are consistent with these findings in that we have documented a significant barium dissolution during acid treatment of Santa Catalina sediment samples. Further evidence for the presence of this phase is documented by the observation of an increase in dissolved barium in pore waters extracted from cores that have been stored at *in situ* temperatures for a few hours after recovery (Figure

2.11). This pore water artifact was also apparent when comparing benthic barium fluxes from pore waters extracted several hours after core recovery with measurements using benthic incubation chambers (McManus et al., 1998). Although these authors clearly document the presence of a labile barium-bearing phase, there were no characterization of the solid phase to explain these observations.

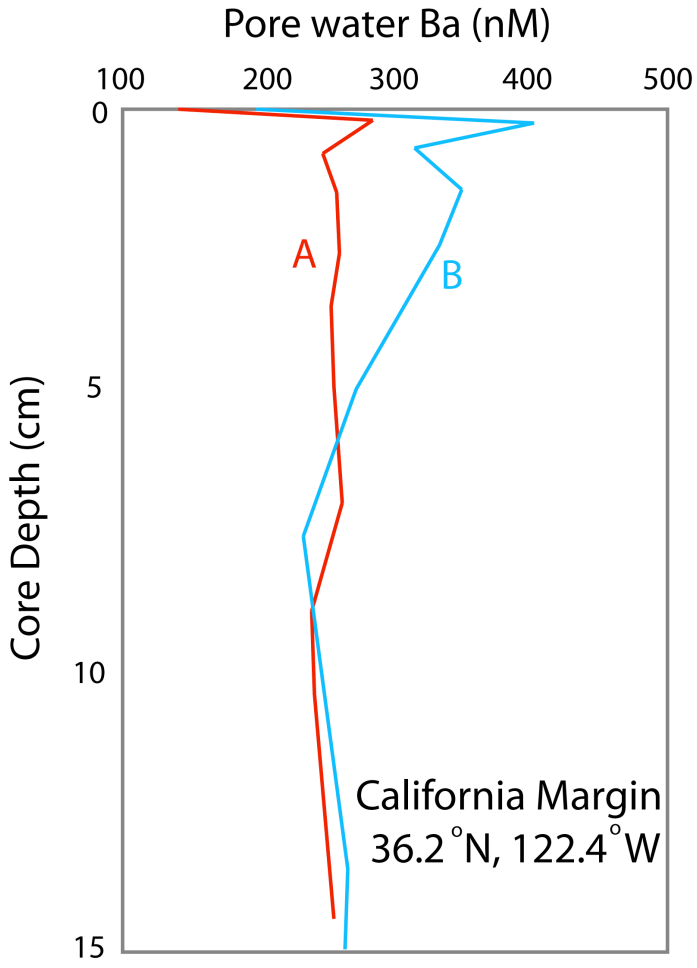

Figure 2.11. Porewater profiles demonstrating the presence of the high Ba labile phase in the surface sediments, which easily dissolves, releasing Ba to the porewater if sample processing is delayed (modified plot from McManus et al., 1998). Both cores were collected from the same multi-core deployment and were stored in a cold room at in situ temperatures upon recovery, whereas core B (blue) was processed 4 hours after core A (red).

2.4.3 Hydroxylamine leach

During this step of the procedure ~7% of Ba dissolved for barite; the fraction of barium leached with this mildly reducing treatment is similar in both the Santa Catalina and San Clemente sediments (~4%). However, by comparing the distribution on the barium peak with that of iron, we clearly see that in these two basins, barium is associated with different carrier phases (Figure 2.12). We observed similar chromatogram shapes for barite (Figure 2.12A) and San Clemente sediment (Figure 2.12B) in the hydroxylamine leach, with Sr/Ba ratios of 69 mmol/mol and 75 mmol/mol, respectively, indicating that Ba in San Clemente sediment is dominated by barite. The Santa Catalina sediment has significantly less barium than the San Clemente sample (Table 2.8) but has instead a significant component of Fe oxyhydroxides that are diagenetically remobilized in the upper 10 cm of the sediment (McManus et al., 1999). These independent findings are consistent with our FT-TRA results (Figure 2.12B and 2.12C), which show a synchronous release of barium and iron only for the Santa Catalina sediments. In the barite-dominated sample from San Clemente, barium dissolution follows the iron peak, revealing that oxhyhydroxides do not sinificantly contribute to the barium inventories of these sediments.

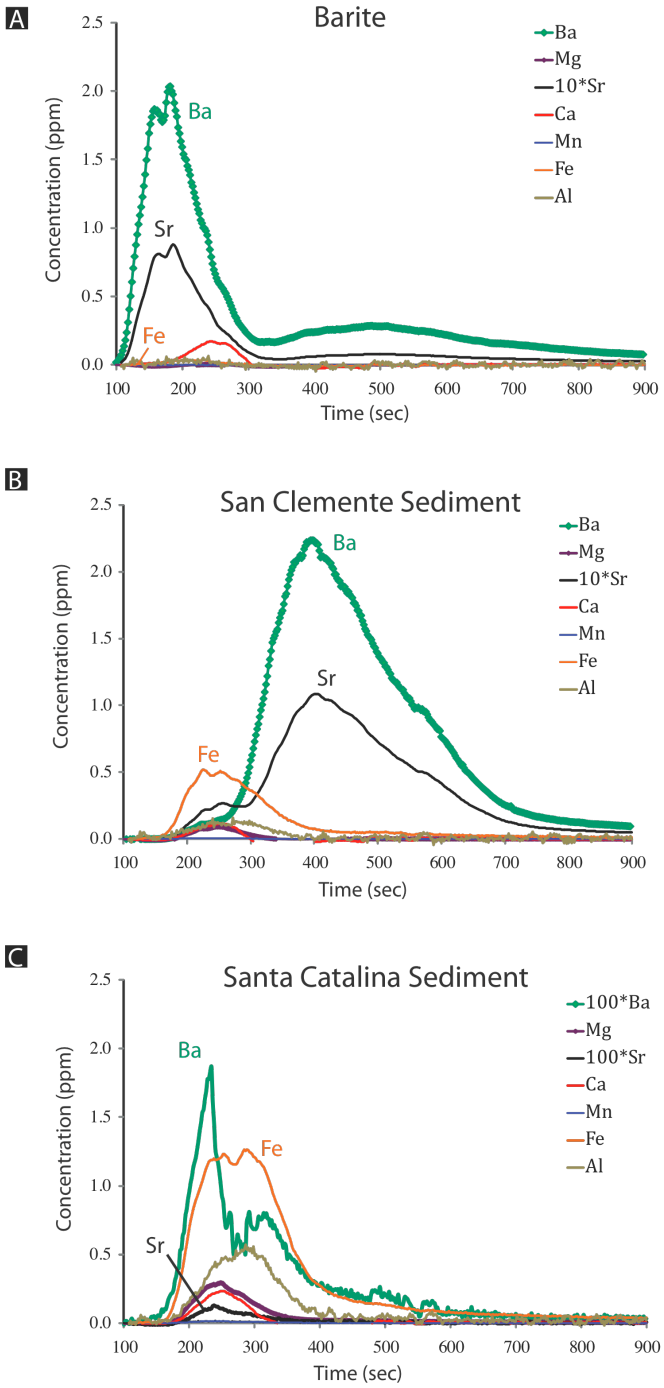

Figure 2.12. Chromatograms of FT-TRA data in the beginning 15 minutes from barites, San Clemente sediments and Santa Catalina sediments leached with acidic NH_2OH.

2.4.4 DTPA leach

Chromatograms of barite and San Clemente sediment leached with DTPA and their Sr-Ba plots are shown in Figure 2.13. Approximately 80% of all barium dissolution occurred in DTPA for both barite and San Clemente sediment. We observed very similar Ba and Sr chromatograms in the barite (Figure 2.13A) and sediment (Figure 2.13B) samples. Both had high Sr/Ba ratio in the beginning of 10 minutes, which fell to a nearly constant ratio by the end of experiment. The high-Sr phase at the beginning of DTPA barite treatment was ~70 mmol/mol, but this value eventually leveled off to a constant ratio of 42 mmol/mol in the last 20 minutes. The same Sr/Ba phases have been observed for barite in both the hydroxylamine and DTPA leaches indicating that barite samples contain several distinct phases. Sr/Ba in San Clemente sediment at the beginning of DTPA treatment starts at ~300 mmol/mol and then drops to a constant ratio of 67 mmol/mol. This phase has also been observed in the acid leach of this sediment suggesting that the bulk of the Sr resides in a high-Sr carbonate phase.

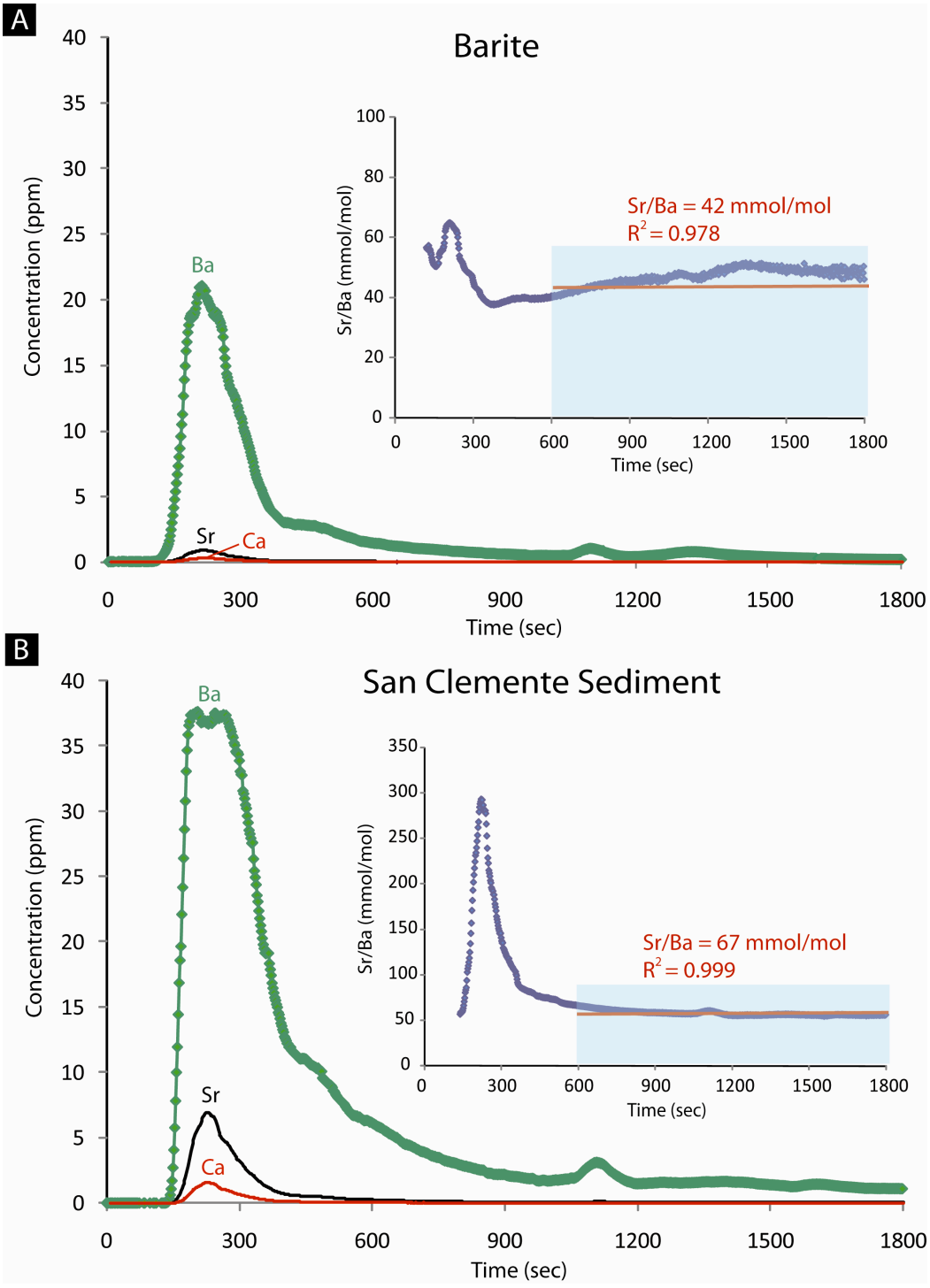

Figure 2.13. Chromatograms of FT-TRA data from barites and San Clemente sediment leached with DTPA. Barite has similar chromatogram shapes with San Clemente sediment, indicating that San Clemente sediment is dominated by barite. Both samples have ~80% of total Ba dissolution in the DTPA leach.

2.5 Conclusions

A comparative analysis of several key elements during FT-TRA of marine barite and sediment samples documents the great potential of this technique to identify various barium carrier phases, their composition ranges and their potential behavior during early sediment diagenesis. We are aware of the myriad of potential complications that arise from the sequential leaching of complex mixtures, the results shown here have revealed the presence and composition of previously unrecognized phases in marine samples. We clearly documented the Sr variability in marine barites and showed the presence of a highly soluble Sr-rich phase with Sr/Ba ratios ranging from 90 to 210 mmol/mol in the beginning 3 minutes of DIW treatment, followed by a lower-Sr less soluble phase with ratios of 30-60 mmol/mol. The high-Sr phase contributes <1% of the total Ba, but its high solubility means that it has been totally missed by previous batch experiments.

Applications of FT-TRA on San Clemente and Santa Catalina sediments help us better understand the roles of different barium carriers. Comparison of Sr, Ba and Ca of these sediments with the expected barite and foraminifera end-members revealed the presence of an additional carbonate phase in both San Clemente and Santa Catalina basins, and this phase was shown to contribute ~50% of the total barium in Santa Catalina sediment. We postulate that this phase represents the hitherto unrecognized labile barium phase, which was inferred to be present in hemipelagic sediments based on pore water distributions (McManus et al., 1998). Because the San Clemente sediments are dominated by barite, the total contribution of the carbonate phase to the total barium inventories in this basin is negligible. For

San Clemente sediment as well as for barite samples, the main fraction of the barium is released during the leaches with DTPA, as expected.

San Clemente sediment has similar chromatogram shapes and Sr/Ba ratios with barite in the acidic NH_2OH leach, consistent with the fact that San Clemente sediment is dominated by cold-seep barites. Santa Catalina sediment, on the other hand, has very small amount of Ba (~0.14%) but has a significant fraction of Fe oxyhydroxides that are diagenetically remobilized in the upper sediments (McManus et al., 1999). The association of barium with oxyhydroxides is postulated based on a synchronous release of Fe and Ba in the chromatograms of FT-TRA during the acidic NH_2OH leach, which is consistent with observations of pore water data published for this basin.

Our results demonstrate the great potential of FT-TRA for partitioning barium among different phases in marine sediments. Further analyses using FT-TRA in more sediment samples and end-member carrier phases will be neccessary for a better understanding of the role for each phase in the total inventories and cycling of this element.

2.6 Acknowledgements

We are grateful to Bobbi Conard, June Padman and Bart De Baere for laboratory and analytical assistance and Erica McQuay for letting us use her barite and sediment samples. This project was carried out in W.M. Keck Collaboratory for Plasma Mass Spectrometry at Oregon State University and was supported by NSF-OCE-MGG 0550377 to Gary Klinkhammer and Marta Torres.

Chapter 2

Discovery Using Flow-Through Chemical Leaching: Ba-Rich Secondary Phase Associated with the Biogenic Carbonate Fraction of Marine Sediments

Chih-Ting Hsieh, Gary P. Klinkhammer, Marta E. Torres and Bart De Baere

3.1 Abstract

Foraminifera are common components of marine sediments, and compositional changes in their tests are known to contain a rich record of environmental change. Barium is incorporated into foraminiferal shells via substitution with Ca in the calcite lattice and as such the Ba/Ca ratio has been used as a circulation tracer and as a refractory nutrient proxy. Accurate reconstructions of paleoceanographic records depend on a fundamental understanding of the element's geochemical cycle in the oceans and of underlying processes leading to the trace metal incorporation in the shells of foraminifera and associated phases. Flow-through time-resolved analysis (FT-TRA) coupled with Inductively-Coupled Plasma Mass Spectrometry allows us to elucidate changes in the elemental distributions associated with calcite tests based on mineral phase susceptibilities to dissolution. Such information provides clues to the mechanisms leading to the observed ratios and to the potential roles of the associated phases in elemental cycling. Samples collected from the South Pacific show a homogeneous Ba distribution within the shell, and Ba/Ca ratios that are consistent with those expected from live culture experiments. In contrast, samples from the Equatorial Pacific show a significant amount of excess barium (>90%) associated with a secondary phase (overgrowth) that is leached from the shell after most of the biogenic calcium has dissolved. In the carbonate-rich Equatorial Pacific this acid-soluble phase contributes ~8% of total sedimentary barium.

3.2 Introduction

Barium is known to mimic silica in the oceans (Chan et al., 1977) and to be incorporated into foraminiferal shells via substitution with Ca in the lattice site (Lea and Boyle, 1990; Lea and Boyle, 1991). The close relationship between Ba and Si in the water column has led to the use of foraminiferal Ba/Ca ratio as a paleotracer of circulation (Lea and Boyle, 1989; Lea and Boyle, 1990a, 1990b; Lea and Boyle, 1991; Lea, 1993). Culture experiments conducted by Lea and Spero (1994) showed that the Ba content in foraminiferal shells is positively correlated with Ba/Ca ratios in the seawater medium. The Ba/Ca ratio in foraminiferal shells has also been used as a potential indicator of changes in glacial meltwater discharge to the Arctic Ocean (Hall and Chan, 2004).

The utilization of Ba/Ca as a paleoproxy hinges on the assumption that all Ba in the biogenic tests is incorporated during calcification with Ba/Ca ratios that are positively correlated with the Ba/Ca in seawater. It is clear, however, that in many cases additional barium phases may be present in the foraminifera that obscure the biogenic ratios (Lea and Boyle, 1989, 1990, 1991, 1993). These authors suggest the use of a series of cleaning approaches to chemically and/or physically remove barium-rich coatings, barite and other non-biogenic phases present in foraminifera pointing out that the presence of these secondary phases may be responsible for complications in the record preserved in the foraminiferal shells recovered from the old sediments.

The development of Flow-Through Time-Resolved Analysis (FT-TRA), an automated leaching technique, coupled with Inductively Coupled Plasma-Mass

Spectrometry (ICP-MS) constitutes a powerful tool for further investigating the composition of the phases associated with biogenic calcite in unprecedented detail (Haley and Klinkhammer, 2002). For example, Hoogakker et al. (2009, in press) used this technique to successfully separate the primary foraminiferal calcite from high Mg-calcite in samples collected from the highly saline Red Sea.

In this study we use FT-TRA to analyze foraminiferal samples from widely distributed oceanic sites, and show that in regions characterized by high barium flux to the sediment, a significant component of the total Ba associated with biogenic calcite is not in the primary phase but instead associated with a secondary phase (overgrowth). Foraminifera from Equatorial Pacific sediments are particularly enriched in this phase, with more than 90% of the carbonate-bound barium occurring in the nonbiogenic phase. In these carbonate-rich sediments, this acid-soluble secondary phase contributes ~8% of total sedimentary barium. Chemical evidence and mass balance considerations lead us to conclude that this secondary phase is a carbonate and not labile barite. While the exact nature of this phase has yet to be determined there is no doubt that its mere presence complicates the use of foraminiferal Ba/Ca as a paleoproxy but also opens the door for future development.

3.3 Materials and Methods

We examined foraminiferal samples from several sites in the Equatorial Pacific and compared our results with similar results from other locations using core-top sediment samples from Oregon State University Marine Geology Core Repository (Figure 3.1, Table 3.1). Freeze-dried sediment samples were suspended in Calgon (sodium hexametaphosphate) and shaken for 20 minutes. The slurries were then transferred to a 125-μm sieve and carefully rinsed with deionized water (DIW) to remove all the clay. The coarse fraction was dried in the oven at 35-40°C overnight. Foraminiferal tests were handpicked under a microscope; only intact shells were selected for our experiments.

Table 3.1 List of foraminiferal samples in this study, site locations shown in Figure 3.1

Sample ID	Latitude	Longitude	Water depth (m)	Species	% $CaCO_3$	Ba in sediment (ppm)
West Africa						
Circe 220PG	-7.567	-1.532	4408	*G. ruber*	--	250
Circe 224P	-7.688	-6.357	4808	*G. ruber*	--	
Circe 228G	-7.825	-6.47	4533	*G. ruber*	--	
Circe 277G	-7.813	-6.24	4281	*G. ruber*	--	
Arabian Sea						
TTN041-11MCB	17.435	58.812	3618	*G. ruber*	38%	890
South Pacific						
KN7812-17BC	-49.552	-179.702	2990	*G. ruber*	--	130
S. E. Pacific						
RR9702A-60MC7	-20.878	-81.499	2480	*G. ruber*	--	960
Eastern Equatorial Pacific						
202-1238B-1H-1, 88-90 cm	-1.87	-82.78	2203	*G. ruber*	>50%	--
202-1238B-1H-3, 40-42 cm	-1.87	-82.78	2203	*G. ruber*	>40%	--
ME0005A-17JC	4.61	-86.70	905	Mixed species[a]	88%	500
Equatorial Pacific						
TTN013-112MC8	5.0783	-139.6383	4418	*G. ruber* and *G. sacculifer*	80-85%	1390
TTN013-82MC6	2.0633	-140.15	4413	*G. ruber*		1980
TTN013-88MC4	0.815	-139.9167	4415	*G. ruber*		1790

[a] *G. ruber*, *N. dutertrei*, *G. sacculifer*, *F. menardii*, *G. glutinata*, *G. tumida* and *O. universa*

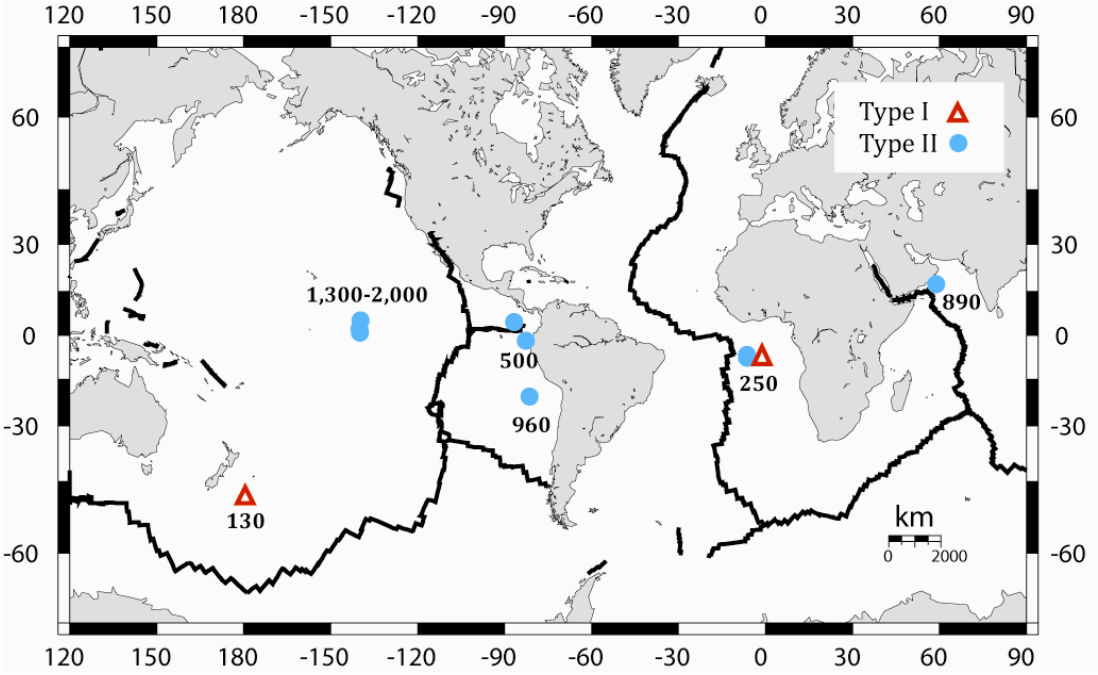

Figure 3.1. Maps of core locations for the foraminifera samples used in this study. Type I denotes samples in which most of the barium is associated with a primary biogenic signal; Type II denotes samples that are dominated by a secondary Ba-rich carbonate phase. The numbers next to the symbols represent the total Ba contents of the sediment at that location in parts-per-million. Type I samples are typically found in sediments with <300 ppm Ba—those containing mostly detrital barium. Type II foraminiferal samples are typically found in sediments enriched in Ba (500-2000 ppm).

Foraminiferal samples were analyzed using FT-TRA coupled with ICP-MS. This automated chromatographic technique uses an integrated leaching module built from a combination of off-the-shelf Dionex chromatographic components, chemically inert digitally controlled valves, and custom-built integrated control circuits. A Dionex Advanced Gradient Pump (AGP) Module provides a continuous flow of eluate with precisely controlled composition, flow rate and pressure. The eluate passes through a heater that maintains it at a constant temperature, which in the case of these foraminiferal analyses was set at 80 ± 2 °C. The eluate then passes from the

sampling column into a mixing tee, where it is combined with 2M HNO_3 spiked with a pre-mixed internal standard of In-115, which is used to correct for fluctuations in the plasma. Additional valves in the system allow for the incorporation of rinsing steps within the analytical procedure, as well as for the injection of standard solutions to generate calibration curves.

The first step in our FT-TRA method was a 2-minute rinse step with DIW to remove any loosely bound coating. Initially samples were leached with 10 mM HNO_3 for 30 to 40 minutes, which was long enough to dissolve most biogenic calcite. However, in some samples we observed a dramatic increase in Ba after most of the biogenic carbonate phase had dissolved (Figure 3.2A and 3.2B), i.e. after the Ca concentration had reached a maximum and started to decrease. To further resolve this later-stage Ba peak, we selected two samples composed of foraminiferal shells randomly picked from Equatorial Pacific core-top sediments (ME0005A-17JC, Table 3.1) and extended the acid leach. We also modified the FT method to leach the shells with DIW brought up to pH 8 with NH_4OH. These samples were leached with DIW for 10 minutes, followed by dissolution with nitric acid, which was ramped from 0 to 3 mM over 10 minutes and then kept at 3 mM for another 3 to 3.5 hours. As typical with FT-TRA the eluates in these extended leaches were continuously monitored and leaching terminated only after most of the acid-leachable barium was removed, which required ~4 hours of total analysis time.

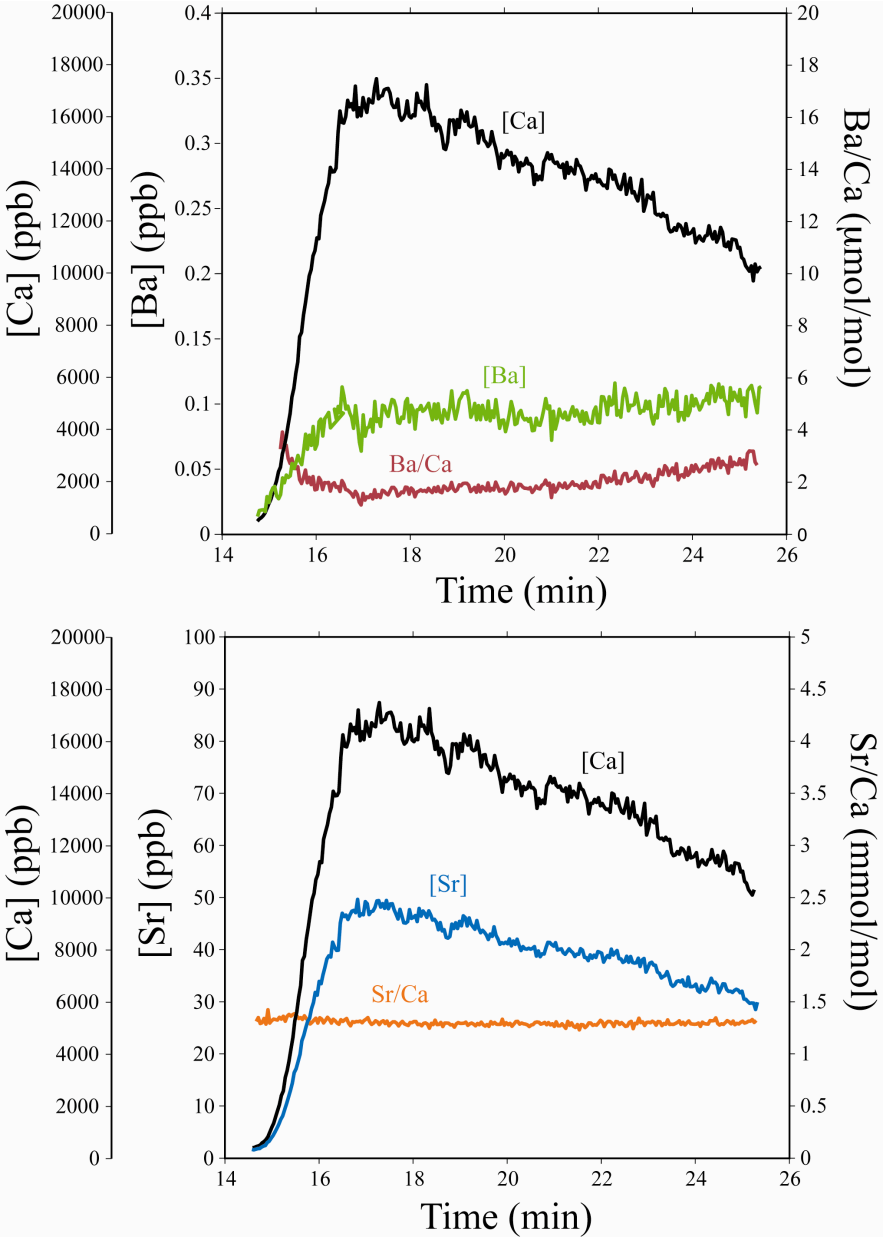

Figure 3.2. Dissolution chromatograms of a sample of 10 foraminiferal shells (*G. ruber*) from a core top recovered from the South Pacific (KN7812-17BC in Tables 1 and 2), showing (A) calcium, barium and Ba/Ca ratio and (B) calcium, strontium and Sr/Ca ratio as samples are leached with HNO_3. This is an example of what we are calling a Type I sample with a biogenic Ca-weighted Ba/Ca ratio of 1.7 µmol/mol averaged and no secondary barium phase. Figure B shows that Sr is also distributed homogeneously in these shells with a Sr/Ca ratio of 1.3 mmol/mol.

3.4 Results and Discussion

Sr/Ca_{bio} and Ba/Ca_{bio} ratios (Ca-weighted) most representative of biogenic calcite were gleaned from the TRA chromatograms by selecting the section under the Ca peak that gave the lowest standard error. Average ratios selected this way from FT-TRA can be significantly different than ratios determined by traditional batch processing analyses, which would be equivalent to the Ca-weighted average of all ratios in the chromatogram, assuming the chemical method was the same. The Ca-weighted biogenic ratio from FT-TRA is calculated using a Matlab-based software program, which defines the Ba/Ca_{bio} as the following:

$$\frac{Ba}{Ca}_{bio} = \frac{\Sigma([Ca]_x \times (Ba/Ca)_x)}{\Sigma[Ca]_{o-t}} \quad (1)$$

where $[Ca]_x$ and $(Ba/Ca)_x$ are the calcium concentration and Ba/Ca at time x in the selected section of ratios, respectively. $[Ca]_{0\text{-}t}$ denotes the integrated calcium concentration.

This approach allows the analyst to select ratios from a time-slice of the dissolution chromatogram. This slice typically contains several hundred ratios whereas in traditional batch processing the sample is dissolved prior to analysis and produces a single ratio per sample. The FT-TRA results for samples of *G. ruber* analyzed for this work are summarized in Table 3.2.

Table 3.2. Data summary for FT-TRA of *G. ruber* samples in our study. Type I are defined as those where barium was present only as a primary biogenic phase. Type II are those that showed a secondary, acid-soluble overgrowth phase. Literature values for biogenic ratios are 1.16-1.50 mmol/mol[a] and 0.5-5 μmol/mol[b] for foraminiferal Sr/Ca and Ba/Ca, respectively.

Sample ID	Core depth (cm)	Sr/Ca_{bio} (mmol/mol)	std error ($\times 10^{-3}$)	Ba/Ca_{bio} (μmol/mol)	std error ($\times 10^{-5}$)	$Ba/Ca_{overgrowth}$ (μmol/mol)
Type 1 (biogenic Ba only)						
West Africa						
Circe 220P	0-1	1.3	2.4	1.2	2.6	None
Circe 224P	2-3	1.3	2.3	1.7	2.3	None
Circe 228G	0-1	1.3	3.0	1.4	2.0	None
South Pacific						
KN7812-17BC	0-5	1.3	1.7	1.7	1.6	None
Type 2 (high-Ba overgrowth)						
West Africa						
Circe 277P	2-3	1.3	3.0	<1.4	4.5	12
Arabian Sea						
TTN041-11MC-B	0-5	1.4	2.7	<2.1	3.9	16
S.E. Pacific						
RR9702A-60MC7	0-1	1.5	7.6	<1.5	27.4	30
Central Equatorial Pacific						
TTN013-112 MC8	1-2	1.3	4.6	<3.0	12.1	>80
	3-4	1.3	4.8	<3.2	11.3	30
	4-5	1.3	7.1	NA[c]	NA[c]	>140
TTN013-88MC4	16-17	1.3	5.1	<1.7	19.6	>20
	19-20	1.3	4.4	<1.2	5.4	10
	27-28	1.4	5.8	<3.2	8.8	>100
	29-30	1.4	4.9	<3.1	7.3	>35
	30-31	1.4	5.2	<3.8	11.0	>100
TTN013-82MC6	15-16	1.4	3.9	<3.7	4.8	>60
	16-17	1.4	3.5	<3.3	5.3	>60
	17-18	1.4	3.2	<3.2	5.1	>80
	18-19	1.4	3.1	<2.8	4.1	>300
	19-20	1.4	4.0	<2.9	4.4	>160
	20-21	1.4	4.2	<2.6	5.6	>800
	21-22	1.3	3.1	<3.2	4.5	>80
	22-23	1.4	3.8	<3.2	5.0	>50
E. Equatorial Pacific						
202-1238B-1H-1	88-90	1.4	6.6	NA[c]	NA[c]	>140
202-1238B-1H-3	40-42	1.3	2.1	NA[c]	NA[c]	>50

[a] Brown and Elderfield, 1996.
[b] Lea and Boyle, 1993.
[c] NA: not available because the biogenic Ba phase cannot be separated from the high-Ba overgrowth phase.

3.4.1 General patterns of Ba/Ca distribution in foraminiferal shells

The total range of Sr/Ca_{bio} for all foraminiferal samples analyzed in this study was 1.3 to 1.5 mmol/mol, consistent with the range for planktonic foraminifera in a larger study (1.16~1.50 mmol/mol) reported by Brown and Elderfield (1996). Our FT results clearly show that strontium in the *G. ruber* is fully associated with biogenic calcium and distributed homogeneously in these shells, otherwise the Sr and Ca peaks would not overlap exactly as they do, nor would Sr-Ca fall on a straight line going through the origin. These relationships can only be explained by homogeneous incorporation of Sr in the calcite matrix.

Ba/Ca ratios in these same samples, however, range from 1.2 μmol/mol off West Africa to >350 μmol/mol in the Equatorial Pacific. Based on these wide-ranging distributions, we classified our samples as two types. Type I shows a constant Ba/Ca ratio during the acid leach with values that fall within previously reported data for clean foraminiferal shells 0.5-5 μmol/mol (Lea and Boyle, 1993). An example of Type I is shown in Figure 2 which shows a sample that produced a constant Ba/Ca ratio of ~1.7 μmol/mol during the entire acid treatment. Samples from South Pacific and most samples from West Africa are classified as Type I. These regions are characterized by moderate to low biological productivity, and these sediments have barium contents of less than ~250 ppm (Table 3.1). In these settings, the foraminiferal shell likely records the Ba concentration in seawater as Ba is incorporated into foraminiferal shells via substitution with Ca in the lattice site during biogenic calcification, as shown in the aquarium experiments of Lea and Spero (1994).

In contrast, samples from the Arabian Sea, the Equatorial Pacific, and one of our samples from West Africa are characterized by the presence of a secondary barium peak and are classified as Type II. Two examples of Type II are shown in Figure 3, illustrating the presence of a high-barium phase that is clearly more resistant to leaching than the biogenic calcite. We believe this secondary phase is a Ba-rich carbonate phase. (We further discuss the nature of this phase in a later section.) The ratio in this high-Ba carbonate-bound phase ($Ba/Ca_{overgrowth}$) ranges from 10 to >350 μmol/mol, opening up the possibility that a significant amount of the total barium exists as this secondary phase.

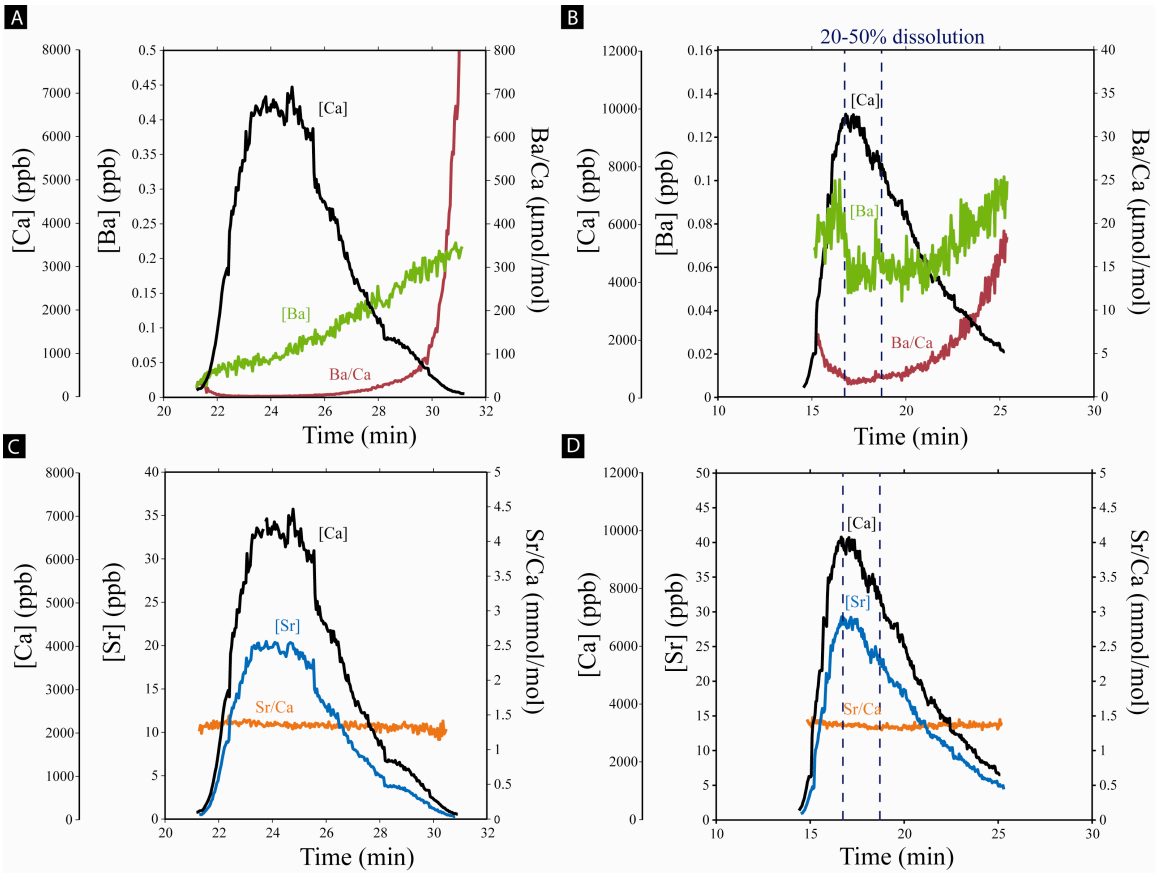

Figure 3.3. Dissolution chromatograms of 10 foraminiferal shells (*G. ruber*) from core tops recovered from the Equatorial Pacific (A and C; TTN013-82MC6 in Tables 3.1 and 3.2), and Arabian Sea (B and D; TTN041-11MC-B in Tables 3.1 and 3.2), showing calcium, barium and Ba/Ca ratios and calcium, strontium and Sr/Ca ratios. The sample on the left is an example of what we call a Type II sample with a reasonable biogenic Ba/Ca ratio of 2.6 µmol/mol and a more resistant overgrowth phase with Ba/Ca ratio >350 µmol/mol. The sample on the right from Arabian Sea is another example of Type II but with less overgrowth leached. C and D show that strontium in these Type II samples is also associated with primary biogenic calcite just as in Type I samples with a Sr/Ca ratio (1.4 mmol/mol).

Barium separation between the primary and secondary phases is typically good enough to allow us to quantify both Ba/Ca ratios. Biogenic Ba/Ca ratios of the foraminifera analyzed for this study range between 1.2 to 3.8 µmol/mol, which are within those reported for pure biogenic calcite (Lea and Boyle, 1993). Some

samples, such as the one from Arabian Sea and one of the samples from West Africa, had reasonable Ba/Ca ratios in the biogenic fraction, but also contained a secondary high-Ba carbonate phase. We found that the sites where Type II foraminiferal samples were collected from had higher Ba contents in the sediment (250-900 ppm) than Type I samples (Table 3.1). In such cases we were able to isolate the biogenic fraction by selecting the sections of the chromatograms that yielded the lowest standard error (provided by the software) of the Ca-weighted average ratios (Figure 3.3B and 3.3D).

In some of the samples from the Equatorial Pacific, we measured extremely high barium in the secondary phase. FT-TRA of these samples, however, do not provide enough peak resolution to separate both phases and the secondary barium contribution (from the overgrowth) masks the biogenic ratio resulting in significantly higher Ba/Ca_{bio} for these samples (Figure 3.3A and 3.3C). These samples have even higher Ba contents in the sediments (>1300 ppm) than the ones we have previously discussed. There were two exceptions from Eastern Equatorial Pacific, with Ba contents of only ~500 ppm in the sediment. When we ran these samples our FT-TRA method failed to separate the biogenic fraction from the overgrowth, which we suspect was due to the contamination of remobilized Ba in the sediment as the samples were not processed immediately after recovery (McManus et al., 1998), but this needs to be tested by additional measuremtns.

In summarym, in our experiments we found a general positive correlation between total Ba content in the sediment and the Ba/Ca ratios of corresponding foraminiferal shells. Although the mechanism is still unknown, early diagenetic

process may have great influence Ba/Ca ratio preserved with biogenic calcite. It is also important to note that the overgrowth phase was more resistant to dissolution in our experiments, which has relevance for proxy methodology.

3.4.2 In depth analysis of barium in foraminiferal samples from the Eastern Equatorial Pacific

To further investigate partitioning of total barium associated with biogenic calcite, we subjected two samples of mixed foraminifera from Eastern Equatorial Pacific (ME0005A-17JC, Figure 3.4) surface sediments to the same FT leaching method but for extended periods of time. We obtained the total element concentrations (Ca_T, Sr_T, Ba_T and Al_T) by integrating FT-TRA chromatograms and normalizing the amounts for each element to In-115 internal standard. By assuming that all Ca_T in these samples comes from the shells and that the Ba/Ca of pristine biogenic calcite ranges from 0.5 to 5 μmol/mol (Lea and Boyle, 1993), we estimated the amount of Ba coming from foraminiferal calcite (Ba_{bio}) in μg using Eq. (2).

$$Ba_{bio} = Ca_T \times \left(\frac{Ba}{Ca}\right)_{bio} (\mu mol/mol) \times 10^{-6} \times \frac{138}{40} \qquad (2)$$

According to Dymond et al. (1992), the amount of Ba contributed from the clay can be corrected using a Ba/Al ratio of 0.0075 mol/mol.

$$Ba_{clay} = Al_T \times \left(\frac{Ba}{Al}\right)_{clay} \times \frac{138}{27} \qquad (3)$$

The excess barium in the foraminiferal shells (secondary carbonate-bound barium) was then estimated using the following equation.

$$Ba_{xs} = Ba_T - Ba_{bio} - Ba_{clay} \quad (4)$$

We calculated a similar mass balance for strontium. Our results show that Ba contributed from the clay is negligible and that 100% of the strontium can be accounted for in the primary biogenic calcite phase, whereas, more than 90% of the Ba in the foraminiferal samples is not associated with primary biogenic calcite, but rather occurs as a secondary phase. We also measured total Ba in the sediment sample and found that the previously unrecognized acid-soluble phase associated with foraminiferal shells contributes ~8% of the total barium in the sediment.

Previous investigators had determined that the main carrier of barium to these sediments was barite with only a minor contribution from carbonates (Gonneea and Paytan, 2006). Our results are generally consistent with their findings. However, even though the carbonate-bound Ba is not the main component in the sedimentary Ba inventory, its presence in a phase leachable in weak acid makes it accessible to recycling during early diagenesis. This carbonate-bound Ba phase may also confound interpretations of paleoenvironments based on Ba/Ca ratios of foraminiferal calcite.

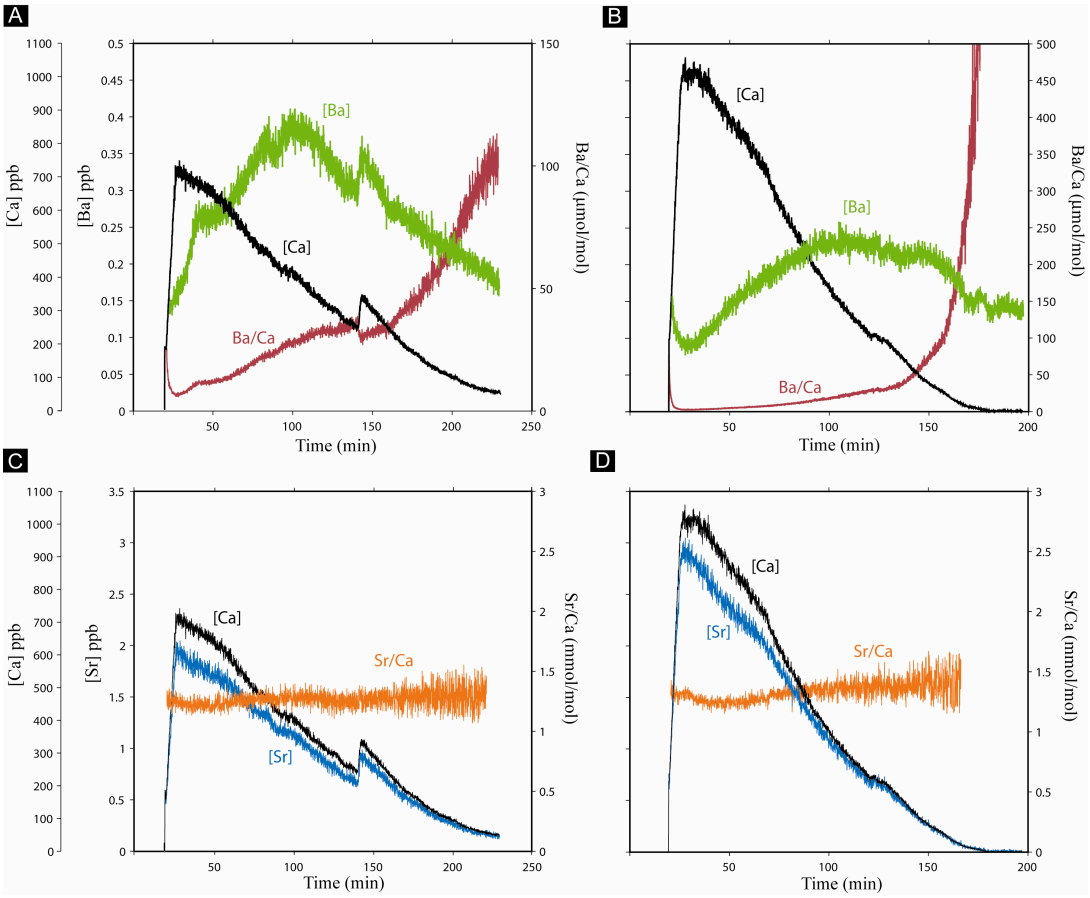

Figure 3.4. Dissolution chromatograms of a sample of mixed foraminiferal shells from core top recovered from the Eastern Equatorial Pacific (ME0005A-17JC). These samples were leached with 3 mM HNO_3 for ~3.5 hours to dissolve most of the secondary barite phase in a Type II sample. (A-B) Show barium, calcium and the Ba/Ca ratios over time. A secondary high-Ba overgrowth is clearly seen A and B with Ba/Ca ratios >100 and > 500 µmol/mol, respectively. We found that more than 90% of the total carbonate-bound barium occurs in the secondary phase. (C-D) Show strontium, calcium and the Sr/Ca ratios over time. In contrast to the barium distribution, strontium is associated with primary biogenic calcite at a constant ratio of 1.3 mmol/mol in these samples.

3.4.3 Potential sources of Ba in the secondary carbonate phase

There are three possible sources of the excess Ba we found to be associated with foraminiferal calcite: (1) Ba bound to the organic matrix that forms the template

for biogenic calcite (2) labile Ba in Sr-rich barite and (3) a separate Ba-carbonate phase. In this section we explore the likelihood of each of these sources.

3.4.3.1 Organic Carbon in the Shell Matrix

A previous FT-TRA study by Haley et al. (2005) proposed that the distribution of the rare earth elements (REEs) in foraminiferal shells could be explained by complexation with the amines used to acquire Ca ions during calcification. This observation is consistent with the high binding efficiency (K_{stab}) of the REEs with proteins and general affinity of these elements for organic carbon, and is further supported by previous work by Martell and Smith (1974) and Lea (1999) who found positive correlation between K_{stab} and the distribution coefficient (K_D) of the REEs, again suggesting that the high REE/Ca ratios in foraminiferal shells might be due to metal complexation with proteins.

While the K_{stab} of Ba is smaller than that of Ca, we cannot totally rule out the possibility that Ba is incorporated into foraminiferal shells by the same mechanism. However we can show by simple calculation that the maximum impact of this process on Ba/Ca would be negligible. To estimate the contribution of Ba via this process, we calculated the maximum amount of Ba in one of our foraminiferal samples from the Eastern Equatorial Pacific (ME0005A-17JC) using Lea's K_D data (1999) and compared it with the total Ba measured in the same sample. This comparison shows that only about 2‰ of the total Ba could be attributed to organic complexation. We conclude from this analysis that organic complexation during

calcification is probably not a major contributor to the carbonate-bound Ba phase observed as “excess Ba” in our experiments.

3.4.3.2 Sr-rich Barite

Although the process controlling barite formation is still unknown, several studies have proposed that barite could be formed in organic-rich microenvironments during the decay of organic matter (Dehairs et al., 1980; Bishop, 1988; Gingele and Dahmke, 1994). In fact Dehairs et al. (1980) suggested that the barite found in upper parts of the oceanic water column may have a Sr/Ba ratio of >200 mmol/mol, which was later documented in the study by Bertram and Cowen (1997) in high productivity areas. Rushdi et al. (2000) provided further support for the presence of high-Sr barite in the upper part of the water column. We are still left with the fact that, while high-Sr barites are highly soluble as shown in this study and would almost certainly dissolve in the water column while sinking, approximately 30% of barite produced in the overlying surface waters is preserved in oxic sediments (Paytan and Kastner, 1996).

Although the mechanism is still not clear, Paytan and Kastner (1996) have suggested that the Sr-rich celestite-barite could be the source of excess Ba in surface sediment. Since most of our foraminiferal samples with a high carbonate-bound barium phase were recovered from the regions of high biological productivity where barites are enriched in the surface sediment (Paytan et al., 1996), we may postulate that another explanation for “excess Ba” we found in the foraminifera is remobilization of barite in the surface sediment.

If this was the primary mechanism giving us the Ba-rich phasse, we would expect to observe a measurable release of Sr associated with the excess Ba during FT-TRA dissolution since Sr-rich barite is known to have a Sr/Ba ratio of between 90 and 260 mmol/mol (Bertram and Cowen, 1997; Chapter 1). However, our FT-TRA results show that the Sr/Ba ratio in the end of acid leaching is approximately 20 times higher than it would be if the Ba was coming from Sr-rich barite. In summary, while our experiments do not rule out the presence of Sr-rich barites, they do suggest that most of excess Ba must be coming from yet another source.

3.4.3.3 Separate Barium-Carbonate Phase

We have shown in our study that Ba/Ca ratio increased in the end of foraminiferal leaching after most of the foraminiferal calcite had dissolved as indicated by Ca, and that these preliminary findings could be explained by the presence of a high-Ba carbonate phase in our samples. Snyder et al. (2007) reported the presence of Ba enrichment in the carbonate extraction step for sediment samples from the Sea of Japan. Moreover our mass balance calculation for strontium show that 100% can be accounted by dissolving primary calcite without invoking another source. We postulate, therefore, that the excess Ba we observed in Equatorial Pacific sediments is most likely associated with a secondary carbonate-bound barium phase. Unraveling its mechanism of formation and its exact chemical composition will require additional FT work using larger samples and additional measurements.

3.5 Summary

We used flow-through time-resolved analysis to resolve two Ba phases commonly associated with foraminiferal samples: (1) primary biogenic barium distributed homogeneously in the calcium carbonate lattice, and (2) a secondary phase more resistant to dissolution than biogenic calcite. This secondary phase seemed to occur more often in highly productive areas with a high Ba flux. We also measured total Ba in the sediment and found that this acid-soluble carbonate phase can contribute up to 8% of the total barium in the sediment. While a relatively small fraction of total sedimentary Ba, this carbonate-bound barium phase is more labile than barite and could be a substantial player during barium diagenesis. Alteration of this secondary fraction downcore could mask the primary Ba/Ca ratio used in paleoceanographic reconstructions. The presence of this hitherto unknown Ba phase needs to be taken into account when trying to isolate the biogenic fraction.

3.6 Acknowledgements

We thank June Padman, Jesse Muratli and Mysti Weber for analytical or/and sample-collecting assistance. We gratefully thank Bobbi Conard and Jack Dymond for letting us use the unpublished Ba data in Arabian Sea and central Equatorial Pacific sediments. This project was carried out in W.M. Keck Collaboratory for Plasma Mass Spectrometry at Oregon State University. Support for this research was funded by grants NSF-OCE-MGG 0426410 to Alan Mix and Gary Klinkhammer and NSF-OCE-MGG 0550377 to Gary Klinkhammer and Marta Torres.

4. Bibliography

Averyt, K. B., and A. Paytan. 2003. Empirical partition coefficients for Sr and Ca in marine barite: Implications for reconstructing seawater Sr and Ca concentrations (May 10). http://www.agu.org/pubs/crossref/2003/2002GC000426.shtml.

Averyt, K. B., A. Paytan, and G. Li. 2003. A precise, high-throughput method for determining Sr/Ca, Sr/Ba, and Ca/Ba ratios in marine barite 4, no. 4 (April 23): 1039.

van Beek, R., Bonte, and Schmidt. 2003. Sr/Ba in barite: a proxy of barite preservation in marine sediments? *Marine Geology* 199, no. 3-4: 205-220.

Bernstein, R. E., and R. H. Byrne. 2004. Acantharians and marine barite. *Marine Chemistry* 86, no. 1-2 (April): 45-50. doi:10.1016/j.marchem.2003.12.003.

Bertram, M., and J. Cowen. 1997. Morphological and compositional evidence for biotic precipitation of marine barite 55, no. 3: 577-593.

Bishop, J. K. B. 1988. The barite-opal-organic carbon association in oceanic particulate matter. *Nature* 332, no. 6162 (March 24): 341-343. doi:10.1038/332341a0.

Boyle, E. 1981. Cadmium, zinc, copper, and barium in foraminifera tests. *Earth and Planetary Science Letters* 53, no. 1 (3): 11-35. doi:10.1016/0012-821X(81)90022-4.

Brown, J. S., and H. Elderfield. 1996. Variations in Mg/Ca and Sr/Ca ratios of planktonic foraminifera caused by postdepositional dissolution: Evidence of shallow Mg-dependent dissolution. *Paleoceanography* 11: 543-552.

Chan, L., D. Drummond, J. Edmond, and B. Grant. 1977. On the barium data from the Atlantic GEOSECS expedition. *Deep Sea Research* 24, no. 7 (7): 613-649. doi:10.1016/0146-6291(77)90505-7.

Collier, R., and J. Edmond. 1984. The trace element geochemistry of marine biogenic particulate matter. *Progress in Oceanography* 13: 113-199.

Church, T. 1979. *Marine Minerals*. R. G. Burns, Ed. (Mineralogical Society of America, Washington, DC, 1979), vol. 6

Dehairs, F., L. Goeyens, N. Stroobants, P. Bernard, C. Goyet, A. Poisson, and R. Chesselet. 1980. On suspended barite and the oxygen-minimum in the Southern Ocean. *Global Biogeochemical Cycles* 4, no. 1: PAGES 85–102.

Dehairs, F., L. Goeyens, N. Stroobants, P. Bernard, C. Goyet, A. Poisson, R. Chesselet. 1990. On suspended barite and the oxygen-minimum in the Southern Ocean. *Global Biogeochemical Cycles* 4, no. 1: PAGES 85–102.

Dehairs, F., N. Stroobants, and L. Goeyens. 1991. Suspended barite as a tracer of biological activity in the Southern ocean 35, no. 1-4: 399-410.

Dehairs, F., W. Baeyens, and L. Goeyens. 1992. Accumulation of Suspended Barite at Mesopelagic Depths and Export Production in the Southern Ocean. *Science* 258, no. 5086 (November 20): 1332-1335. doi:10.1126/science.258.5086.1332.

Dunn, K. and T. F. Yen. 1999. Dissolution of Barium Sulfate Scale Deposits by Chelating Agents. *Environmental Science & Technology* 33, no. 16: 2821-2824. doi:10.1021/es980968j.

Dymond, J., E. Suess, and D. Lyle. 1992. Barium in Deep-Sea Sediment: A Geochemical Proxy for Paleoproductivity 7, no. 2: 163-181.

Dymond, J., and R. Collier. 1996. Topical Studies in Oceanography : Particulate barium fluxes and their relationships to biological productivity. *Deep Sea Research Part II* 43, no. 4-6: 1283-1308. doi:10.1016/0967-0645(96)00011-2.

Fagel, N., F. Dehairs, R. Peinert, A. Antia, and L. Andre. 2004. Reconstructing export production at the NE Atlantic margin: potential and limits of the Ba proxy. *Marine Geology* 204, no. 1-2 (February): 11-25. doi:10.1016/S0025-3227(03)00371-2.

Francois, R., S. Honjo, S. J. Manganini, and G. E. Ravizza. 1995. Biogenic Barium Fluxes to the Deep sea: Implications for Paleoproductivity Reconstruction 9, no. 2 (January): 289-303.

Frank, M. 1995. Sediment redistribution versus paleoproductivity change: Weddell Sea margin sediment stratigraphy and biogenic particle flux of the last 250,000 years deduced from 230Thex, 10Be and biogenic barium profiles. *Earth and Planetary Science Letters* 136, no. 3-4 (12): 559-573. doi:10.1016/0012-821X(95)00161-5.

Ganeshram, R. S., R. François, J. Commeau, and S. L. Brown-Leger. 2003. An experimental investigation of barite formation in seawater. *Geochimica et Cosmochimica Acta* 67, no. 14 (7): 2599-2605. doi:10.1016/S0016-7037(03)00164-9.

Gingele, F. and A. Dahmke. 1994. Discrete Barite Particles and Barium as Tracers of Paleoproductivity in South Atlantic Sediments 9, no. 1: 151-168.

Goldberg and Arrhenius. 1958. Chemistry of Pacific pelagic sediments. *Geochimica et Cosmochimica Acta* 13, no. 2-3: 153-212. doi:10.1016/0016-7037(58)90046-2.

Gonneea, M. E., and A. Paytan. 2006. Phase associations of barium in marine sediments. *Marine Chemistry* 100, no. 1-2 (June): 124-135. doi:10.1016/j.marchem.2005.12.003.

Haley, B., and G. Klinkhammer. 2002. Development of a flow-through system for cleaning and dissolving foraminiferal tests. *Chemical Geology* 185, no. 1-2 (April): 51-69. doi:10.1016/S0009-2541(01)00399-0.

Haley, B. A., G. P. Klinkhammer, and A. C. Mix. 2005. Revisiting the rare earth elements in foraminiferal tests. *Earth and Planetary Science Letters* 239, no. 1-2 (October): 79-97. doi:10.1016/j.epsl.2005.08.014.

Hall, J. M., and L.-H. Chan. 2004. Ba/Ca in Neogloboquadrina pachyderma as an indicator of deglacial meltwater discharge into the western Arctic Ocean (March 4). http://www.agu.org/pubs/crossref/2004.../2003PA000910.shtml.

Klump, J., D. Hebbeln, and G. Wefer. 2000. The impact of sediment provenance on barium-based productivity estimates. *Marine Geology* 169, no. 3-4 (October 15): 259-271. doi:10.1016/S0025-3227(00)00092-X.

Lea, D. and E. Boyle. 1989. Barium content of benthic foraminifera controlled by bottom-water composition. *Nature* 338, no. 6218 (April 27): 751-753. doi:10.1038/338751a0.

Lea, D. W and E. A. Boyle. 1991. Barium in planktonic foraminifera. *Geochimica et Cosmochimica Acta.*Vol. 55.

Lea, D. W. and E. A. Boyle. 1990. Foraminiferal reconstruction of barium distributions in water masses of the glacial oceans. *Paleoceanography* 5, no. 5: PAGES 719–742.

Lea, D.W. and E. A. Boyle. 1993. Determination of carbonate-bound barium in foraminifera and corals by isotope dilution plasma-mass spectrometry 103, no. 1-4: 73-84.

Lea, D. W. and H. J. Spero. 1994. Assessing the Reliability of Paleochemical Tracers: Barium Uptake in the Shells of Planktonic Foraminifera 9, no. 3.

Martell and Hancock. 1996. *metal complexes in aqueous solutions*. Springer.

Martell, A. and R. Smith. 1974. *Critical stability constants,* New York: Plenum Press.

McManus, J., W. M. Berelson, D. E. Hammond, and G. P. Klinkhammer. 1999. Barium Cycling in the North Pacific: Implications for the Utility of Ba as a Paleoproductivity and Paleoalkalinity Proxy. *Paleoceanography*. 14, no. 1: 53-61.

McManus, J., W. M. Berelson, G. P. Klinkhammer, K. S. Johnson, K. H. Coale, R. F. Anderson, N. Kumar, et al. 1998. Geochemistry of barium in marine sediments: implications for its use as a paleoproxy. *Geochimica et Cosmochimica Acta* 62, no. 21-22 (November): 3453-3473. doi:10.1016/S0016-7037(98)00248-8.

McQuay, E. L., M. E. Torres, R. W. Collier, C.-A. Huh, and J. McManus. 2008. Contribution of cold seep barite to the barium geochemical budget of a marginal basin. *Deep Sea Research Part I: Oceanographic Research Papers* 55, no. 6 (6): 801-811. doi:10.1016/j.dsr.2008.03.001.

Paytan, A. and M. Kastner. 1996. Benthic Ba fluxes in the central Equatorial Pacific, implications for the oceanic Ba cycle. *Earth and Planetary Science Letters* 142, no. 3-4 (August): 439-450. doi:10.1016/0012-821X(96)00120-3.

Paytan, A., M. Kastner, E. E. Martin, J. D. Macdougall, and T. Herbert. 1993. Marine barite as a monitor of seawater strontium isotope composition. *Nature* 366, no. 6454 (December 2): 445-449. doi:10.1038/366445a0.

Paytan, A., W. S. Moore, and M. Kastner. 1996. Sedimentation rate as determined by 226Ra activity in marine barite. *Geochimica et Cosmochimica Acta* 60, no. 22 (November): 4313-4319. doi:10.1016/S0016-7037(96)00267-0.

Paytan, A., M. Kastner, D. Campbell, and M. H. Thiemens. 1998. Sulfur Isotopic Composition of Cenozoic Seawater Sulfate. *Science* 282, no. 5393 (November 20): 1459-1462. doi:10.1126/science.282.5393.1459.

Putnis, A., J. L. Junta-Rosso, M. F. Hochella, and Jr. 1995. Dissolution of barite by a chelating ligand: An atomic force microscopy study. *Geochimica et Cosmochimica Acta* 59, no. 22 (November): 4623-4632. doi:10.1016/0016-7037(95)00324-X.

Reitz, A., K. Pfeifer, G. J. de Lange, and J. Klump. 2004. Biogenic barium and the detrital Ba/Al ratio: a comparison of their direct and indirect determination. *Marine Geology* 204, no. 3-4 (March 30): 289-300. doi:10.1016/S0025-3227(04)00004-0.

Rushdi, A. I., J. McManus, and R. W. Collier. 2000. Marine barite and celestite saturation in seawater. *Marine Chemistry* 69, no. 1-2 (March): 19-31. doi:10.1016/S0304-4203(99)00089-4.

Rutsch, H.-J., A. Mangini, G. Bonani, B. Dittrich-Hannen, P.W. Kubik, M. Suter, and M. Segl. 1995. 10Be and Ba concentrations in West African sediments trace productivity in the past. *Earth and Planetary Science Letters* 133, no. 1-2 (June): 129-143. doi:10.1016/0012-821X(95)00069-O.

Rutten, A., and G. J. de Lange. 2002. A novel selective extraction of barite, and its application to eastern Mediterranean sediments. *Earth and Planetary Science Letters* 198, no. 1-2 (April): 11-24. doi:10.1016/S0012-821X(02)00498-3.

Schroeder, J. O., R. W. Murray, M. Leinen, R. C. Pflaum, and T. R. Janecek. 1997. Barium in Equatorial Pacific Carbonate Sediment: Terrigenous, Oxide, and Biogenic Associations 12, no. 1: 125-146.

Snyder, G. T., Akihiro Hiruta, Ryo Matsumoto, Gerald R. Dickens, Hitoshi Tomaru, Rika Takeuchi, Junko Komatsubara, Yasushi Ishida, and Hua Yu. 2007. Topical Studies in Oceanography : Pore water profiles and authigenic mineralization in shallow marine sediments above the methane-charged system on Umitaka Spur, Japan Sea. *Deep Sea Research Part II* 54, no. 11-13 (June): 1216-1239. doi:10.1016/j.dsr2.2007.04.001.

Sternberg, E., D. Tang, T.-Y. Ho, C. Jeandel, and M.M. François. 2005. Barium uptake and adsorption in diatoms. *Geochimica et Cosmochimica Acta* 69, no. 11 (June 1): 2745-2752. doi:10.1016/j.gca.2004.11.026.

Torres, M. E., J. McManus, and C.-A. Huh. 2002. Fluid seepage along the San Clemente Fault scarp: basin-wide impact on barium cycling. *Earth and Planetary Science Letters* 203, no. 1 (October): 181-194. doi:10.1016/S0012-821X(02)00800-2.

Appendix

1. Tables of experiments on marine (cold seep) barite

Spl #	Date (M/D/Y)	DIW		HNO_3			pH 10 NH_2OH			pH 10 DTPA			Comment/sequence
		Flow (ml/min)	Time (min)	concn	flow	time	concn	flow	time	concn	flow	time	
1	07/30/07	1.8	2	500 μM	1.8	118							DIW-HNO_3
	07/31/07	1.8	2	500 μM	1.8	30				0.1 M	0.2	118	HNO_3-DIW-DTPA
	08/01/07									0.1 M	0.2	30	Didn't rinse system between samples
2	08/07/07	1.8	5	500 μM	1.8	25	0.5 M	0.2	119				DIW-HNO_3-rinse-NH_2OH
	08/08/07									0.1 M	0.2	119	Rinse-DTPA
2	08/24/07	1.8	30										DIW, Sit overnight
	08/25/07	1.8	29	0-10 mM	1.8	25							DIW-rinse-HNO_3
				10 mM	1.8	5							
	08/26/07			10 mM	1.8	29	0.5 M	0.2	30				HNO_3-rinse-NH_2OH
	08/27/07						0.5 M	0.2	29	0.1 M	0.2	30	NH_2OH-rinse-DTPA
	08/28/07									0.1 M	0.2	30	DTPA
1	09/01/07	1.8	30										DIW, sit overnight
	09/02/07	1.8	10	0-100 mM	1.8	25							DIW- rinse-HNO_3 ramping up for 25 mins and 100 mM for 5 hours, sit overnight
				100 mM	1.8	240							

Continued from last page

Spl #	Date (M/D/Y)	DIW		HNO_3			pH 10 NH_2OH			pH 10 DTPA			Comment/sequence
		Flow (ml/min)	Time (min)	concn	flow	time	concn	flow	time	concn	flow	time	
	09/03/07			100 mM	1.8	29				0.1 M	0.2	300	HNO_3-rinse-DTPA
9	09/05/07	1.8	5										See if there is a high-Sr peak in the beginning dissolving in DIW.
3	09/30/07	1.8	30										DIW for 30 min. Done.

Spl #	Date (M/D/Y)	pH 7 neutralized DIW (brought up by NH_4OH)		HNO_3			pH 10 NH_2OH			pH 10 DTPA			Comment/sequence
		Flow (ml/ min)	Time (min)	concn	flow	time	concn	flow	time	concn	flow	time	
1	10/16/07	0.2	30										pH7 neutralized water, brought up by ammonium hydroxide
3	04/23/08	0.2	30										Results are corrected by Na

Spl #	Date (M/D/Y)	pH 8 DIW (brought up by $(NH4)_2CO_3$)		HNO_3			pH 10 NH_2OH			pH 10 DTPA			Comment/sequence
		Flow (ml/ min)	Time (min)	concn	flow	time	concn	flow	time	concn	flow	time	
11	09/15/08	0.2	10										pH8 DIW, brought up by ammonium carbonate

Spl #	Date (M/D/Y)	DIW		HNO_3			acidic NH_2OH (25% CH_3COOH)			pH 10 DTPA			Comment/sequence
		Flow (ml/ min)	Time (min)	concn	flow	time	concn	flow	time	concn	flow	time	
1	02/27/09	1.8	2										DIW
	02/28/09	1.8	2	0-3 mM	1.8	25							DIW-HNO_3
				3 mM	1.8	5							
	03/01/09			3 mM	1.8	29	0.02 M	0.2	30				HNO_3-NH_2OH
	03/02/09						0.02 M	0.2	29	0.1	0.2	30	NH_2OH-DTPA
	03/03/09									0.1	0.2	30	DTPA
1	04/28/09	1.8	2										DIW
	04/29/09	1.8	2	0-3 mM	1.8	25							DIW-HNO_3
				3 mM	1.8	5							
	04/30/09			3 mM	1.8	29	0.02 M	0.2	30				HNO_3-NH_2OH
	05/01/09						0.02 M	0.2	29	0.1	0.2	30	NH_2OH-DTPA
	05/02/09									0.1	0.2	30	DTPA

2. Tables of experiments on sediments and foraminiferal shells

@ --San Clemente (7AD 3534 PC 14 #1-3)

$ -- Santa Catalina (NH0312-4mc2-01 0-1 cm)

&--Equatorial Pacific core-top sediment (TTN013-69MC1 0-1 cm)

%--Foraminiferal shells from E. Equatorial Pacific (ME0005A-17JC)

Spl #	Date (M/D/Y)	DIW		HNO_3			pH 10 NH_2OH			pH 10 DTPA			Comment/sequence
		Flow (ml/ min)	Time (min)	concn	flow	time	concn	flow	time	concn	flow	time	
3@	09/17/07	1.8	30										DIW, sit overnight
	09/18/07	1.8	10	0-3 mM	1.8	25							DIW-rinse-0-3 mM HNO_3 ramping up for 25 mins and 3 mM for 5 mins, sit overnight
				3 mM	1.8	5							
	09/19/07			3 mM	1.8	29	0.5 M	0.2	30				HNO_3-rinse-NH_2OH
	09/20/07						0.5 M	0.2	29	0.1 M	0.2	30	NH_2OH-rinse-DTPA
	09/21/07									0.1 M	0.2	30	DTPA
1@	09/30/07	1.8	30										DIW for 30 mins. Done.
3$	10/02/07	1.8	30										DIW, sit overnight
	10/03/07	1.8	10	0-3 mM	1.8	25							DIW-rinse-0-3 mM HNO_3, sit overnight
				3 mM	1.8	5							
	10/04/07			3 mM	1.8	29	0.5 M	0.2	30				HNO_3-rinse-NH_2OH
	10/05/07						0.5 M	0.2	29	0.1 M	0.2	30	NH_2OH-rinse-DTPA
	100607									0.1 M	0.2	30	DTPA

Spl #	Date (M/D/Y)	pH 7 neutralized DIW (brought up by NH_4OH)		HNO_3			pH 10 NH_2OH			pH 10 DTPA			Comment/sequence
		Flow (ml/ min)	Time (min)	concn	flow	time	concn	flow	time	concn	flow	time	
1@	10/16/07	0.2	30										DIW for 30 mins. Done.
1$	10/16/07	0.2	30										DIW for 30 mins. Done.

Spl #	Date (M/D/Y)	pH 8 DIW (brought up by NH_4OH)		HNO_3			pH 10 NH_2OH			pH 10 DTPA			Comment/sequence
		Flow (ml/ min)	Time (min)	concn	flow	time	concn	flow	time	concn	flow	time	
3&	06/02/08	0.2	30										pH8 DIW, sit overnight
	06/03/08	0.2	10	0-3 mM	1.8	25							pH8 DIW-rinse-0-3 mM HNO_3 ramping up for 25 mins and 3 mM for 5 mins, sit overnight
				3 mM	1.8	5							
	06/04/08			3 mM	1.8	29	0.5 M	0.2	30				HNO_3-rinse-NH_2OH
	06/05/08						0.5 M	0.2	29	0.1 M	0.2	30	NH_2OH-rinse-DTPA
	06/06/08									0.1 M	0.2	30	DTPA
2&	08/04/08	0.2	30										pH8 DIW, sit overnight
	08/05/08	0.2	10							0.1 M	0.2	30	pH8 DIW-rinse-DTPA
	08/06/08			0-3 mM	1.8	25				0.1 M	0.2	29	DTPA-rinse-0-3 mM HNO_3 ramping up for 25 mins and 3 mM for 5 mins, sit overnight
				3 mM	1.8	5							
	08/07/08			3 mM	1.8	30							HNO_3 for 30 mins. Done.

%--Foram from E. Equatorial Pacific (ME0005A-17JC)
These experiments were analyzed by ICP-OES.

Spl #	Date (M/D/Y)	pH 8 DIW (brought up by NH_4OH)		HNO_3			pH 10 NH_2OH			pH 10 DTPA			Comment/sequence
		Flow (ml/ min)	Time (min)	concn	flow	time	concn	flow	time	concn	flow	time	
1%	08/04/08	0.2	30										pH8 DIW, sit overnight
	08/05/08	0.2	10							0.1 M	0.2	30	pH8 DIW-rinse-DTPA
	08/06/08			0-3 mM	1.8	25				0.1 M	0.2	29	DTPA-rinse-0-3 mM HNO_3 ramping up for 25 mins and 3 mM for 5 mins, sit overnight
				3 mM	1.8	5							
	08/07/08			3 mM	1.8	30							HNO_3 for 30 mins. Done.
3%	10/03/08	0.2	30										
	10/04/08	0.2	9	0-3 mM	1.8	25							pH8 DIW-rinse-0-3 mM HNO_3 ramping up for 25 mins and 3 mM for 5 mins, sit overnight
				3 mM	1.8	5							

%--Foram from E. Equatorial Pacific (ME0005A-17JC)
These experiments were analyzed by ICP-MS.
Foram species: *G. ruber, N. dutertrei, G. sacculifer, F. menardii, G. glutinata, G. tumida* and *O. Universa*.

Spl #	Date (M/D/Y)	pH 8 DIW (brought up by NH_4OH)		HNO_3			pH 10 NH_2OH			pH 10 DTPA			Comment/sequence
		Flow (ml/ min)	Time (min)	concn	flow	time	concn	flow	time	concn	flow	time	
2%	11/17/08	0.8	9	0-3 mM	0.8	10							Didn't dissolve all the carbonate phase so need to do it again.
				3 mM	0.8	60							
1%	12/03/08	0.8	9	0-3 mM	0.8	10							74% carbonate phase was dissolved.
				3 mM	0.8	210							
1%	12/03/08	0.8	9	0-3 mM	0.8	10							94% carbonate phase was dissolved. More Ba & Sr were found than we expected in the foram.
				3 mM	0.8	177							

@ --San Clemente (7AD 3534 PC 14 #1-3)
$ -- Santa Catalina (NH0312-4mc2-01 0-1 cm)

Spl #	Date (M/D/Y)	DIW		HNO_3			acidic NH_2OH (25% CH_3COOH)			pH 10 DTPA			Comment/sequence
		Flow (ml/ min)	Time (min)	concn	flow	time	concn	flow	time	concn	flow	time	
1@ 1$	02/27/09	1.8	2										DIW
	02/28/09	1.8	2	0-3 mM	1.8	25							DIW-HNO_3
				3 mM	1.8	5							
	03/01/09			3 mM	1.8	29	0.02 M	0.2	30				HNO_3-NH_2OH
	03/02/09						0.02 M	0.2	29	0.1	0.2	30	NH_2OH-DTPA
	03/03/09									0.1	0.2	30	DTPA
1@ 1$	04/28/09	1.8	2										DIW
	04/29/09	1.8	2	0-3 mM	1.8	25							DIW-HNO_3
				3 mM	1.8	5							
	04/30/09			3 mM	1.8	29	0.02 M	0.2	30				HNO_3-NH_2OH
	05/01/09						0.02 M	0.2	29	0.1	0.2	30	NH_2OH-DTPA
	05/02/09									0.1	0.2	30	DTPA

3. **Chromatograms of five-day experiment on Santa Catalina sediments (042809-050209).**

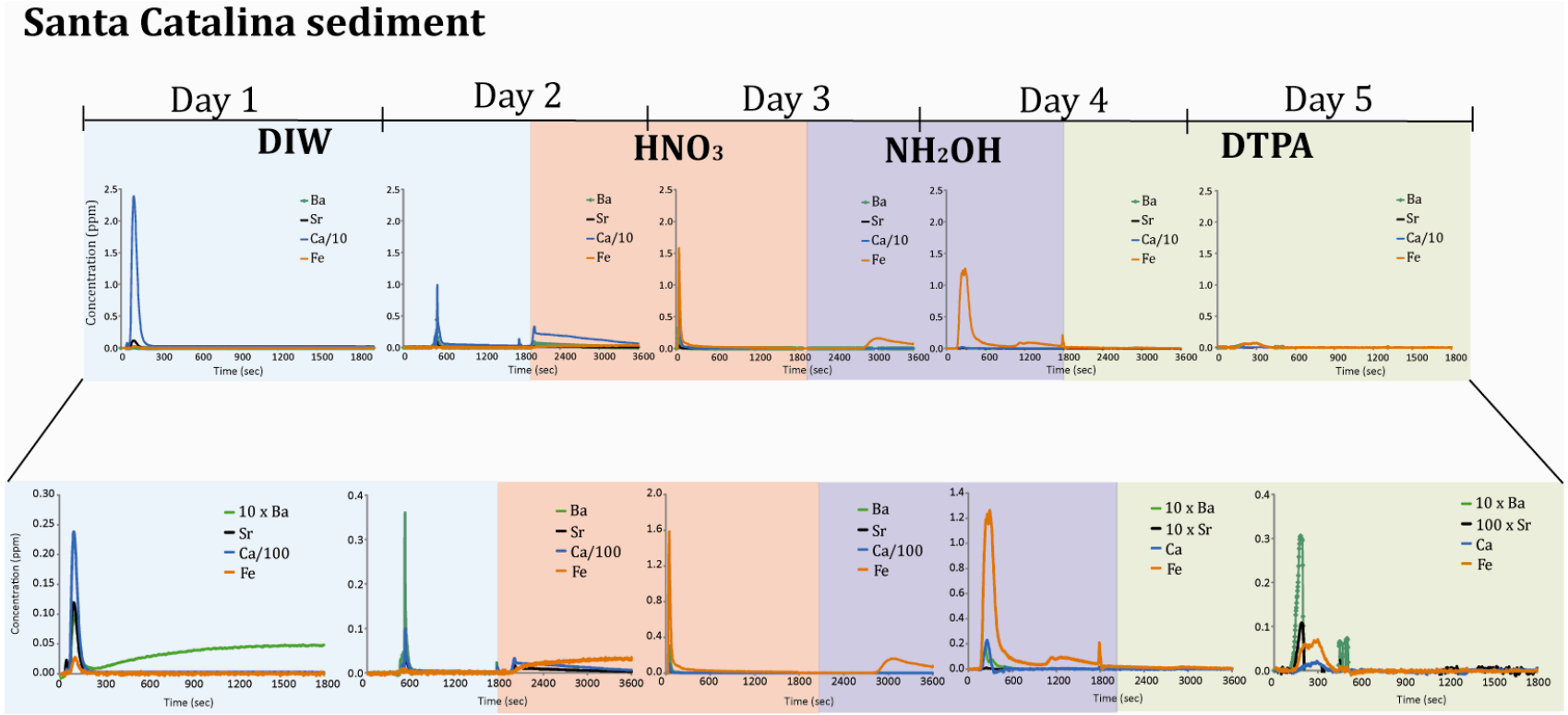

4. **Data and results from Chapter 1 and Chapter 2 are available in the accompanying compact disc (for bound version of thesis).**